Shaping Kale Morphology and Physiology Using Different LED Light Recipes

Sabine Scandola[1,2,*], Lauren E. Grubb[1,*], Brigo Castillo[1], Lexyn Iliscupidez[1], Curtis Kennedy[1,3], Nicholas Boyce[1], and R. Glen Uhrig[1, 4,#]

[1] Department of Biological Sciences, University of Alberta, Edmonton, Alberta, Canada

[2] Lethbridge Research and Development Centre, Agriculture and Agri-Food Canada, Lethbridge, Canada

[3] Department of Computer Science, University of Alberta, Edmonton, Alberta, Canada

[4] Department of Biochemistry, University of Alberta, Edmonton, Alberta, Canada

[*]These authors contributed equally (S.S. and L.G.)

[#] Senior and corresponding author:

Dr. R. Glen Uhrig
Department of Biological Sciences,
University of Alberta,
Edmonton, Alberta, Canada, T6G 2E9
Email: ruhrig@ualberta.ca
Phone: +1 780 492 3088
Fax : +1 780 492-9234ruhrig@ualberta.ca

Running Title: Light condition effects on kale growth and development

Key Words: Kale, Anthocyanins, Light emitting diodes (LEDs), Horticulture, PhotosynQ, Quantitative Proteomics, Metabolomics

Abstract

In the evolving landscape of horticultural science, light emitting diodes (LEDs) present an innovative opportunity for manipulating plant growth and development. Light serves as a fundamental energy source and an environmental cue for plant life, providing us an ability to control essential plant traits through the precise manipulation of light intensity and quality. In this study, we assess the effects of light intensity and spectral composition on the growth and physiology of a horticulturally significant model plant: Kale (*Brassica oleracea*). Selected for its phenotypic plasticity and nutritional composition, kale is a crop well-suited for indoor cultivation using LEDs. Here, we employ a combination of advanced phenotyping, computer vision, gas chromatography-mass spectrometry (GC-MS) metabolomics, and liquid chromatography-mass spectrometry (LC-MS)-based quantitative proteomics to characterize the molecular changes that underpin light-dictated differences in the growth and metabolism of two different kale cultivars under different light intensity and spectral composition scenarios. Our results not only offer a key resource to the plant community, but also demonstrate the translational potential of light manipulation in tailoring kale growth and nutritional content for enhanced crop productivity and/or nutritional content, while simultaneously offering a more cost-effective solution for contemporary agricultural challenges.

1 Introduction

Kale (*Brassica oleracea*), also known as leaf cabbage, belongs to the large *Brassicaceae* family that includes cauliflower, broccoli and collard greens. Established as a superfood, this leafy green is rich in fiber and essential vitamins, as well as antioxidants such as flavonoids, each of which have been shown to positively affect cardiovascular and gastrointestinal health[1–3]. To date, the health benefits of kale have been heavily studied, with researchers continuing to identify new anti-cancer (e.g. sinigrin, spirostanol)[4] and neuroprotective (e.g. sulforaphane)[5] compounds, which neutralize reactive oxygen species. Further, kale demonstrates excellent temperature resilience as a result of its waxy coating and high production of polyamines[6], rendering it a valuable agricultural crop in the context of climate change[7].

Kale is also suited for indoor / vertical farming. As a leafy green, it is a favored choice for horticultural growers as it has a quick harvest cycle with minimal space and resource requirements[8], appealing to both growers as well as consumers looking for fresh, locally-sourced produce[9]. Indoor / vertical farms have strongly co-evolved with new technologies as the promise of providing fresh and locally grown food largely relies on reducing production costs through technological advancements[10,11]. In this context, LED technology has revolutionized indoor farming, providing a wide range of energy-efficient and versatile lighting options. For example, unlike traditional light sources (e.g. incandescent bulbs, fluorescent tubes, metal halide or high pressure sodium bulbs), LED lighting systems offer an ability to fine-tune the spectral composition and intensity of the applied light[12,13]. Light is critical for photosynthesis, which drives plant metabolism and growth[14], while plant photoreceptors, such as phytochromes and cryptochromes, respond to light quality, impacting processes such as plant growth (e.g. biomass) and development (e.g. flowering)[15]. However, despite our understanding of kale at a phenotypic level, we lack knowledge of how light impacts kale at the molecular level, limiting our ability to enhance genetics through targeted breeding or biotechnology approaches.

To date, elementary changes in spectral composition have been shown to affect kale phenotypic and metabolic profiles[16]. Blue light enhances growth and nutritional qualities[17], while red light affects kale pre- and post-harvest by altering metabolites and chlorophyll content[18]. Similar to red light, far-red light enhances photosynthetic rates through the Emerson effect[19]. Beyond specific light types, light wavelength ratios also play an essential role in how phytochromes perceive and transduce light signals[20], offering opportunities to build precise light recipes that maximize traits of interest.

To better exploit currently available kale genetics, we endeavored to precisely resolve the impacts of light intensity and spectral composition on kale growth, development and nutritional content by contrasting the diel molecular changes in two related kale cultivars: Dwarf curled scotch (K3) and Red Scarlet (K9) (**Figure 1**). While there are many kale cultivars, each with unique morphologies, growth parameters and nutritional characteristics[21], our previous study examining nine commercially available kale cultivars found that K3 and K9, both *Brassica oleracea var. sabellica*, showed the most diversity in their phenotypes and molecular characteristics[21], allowing us here to capture an in-depth understanding of how light properties impact kale growth and development in order to establish a compendium of molecular changes that can be utilized by the broader community. We specifically took a diel experimental approach to analyzing the effects of light intensity and spectral composition by harvesting tissues at end-of-day (ED, ZT11 (zeitgeber)) and end-of-night (EN, ZT23) time-points as both the proteome and metabolome are known to undergo substantial diel changes[21]. Understanding how external factors such as time-of-day intersect with differences in light intensity and quality to impact kale physiology, is essential for determining optimal horticultural growing conditions and harvesting times in order to maximize value, as well as inform future efforts in breeding more productive and nutritious kale varieties.

2 Materials and Methods

2.1 Plant material and cultivation

Dwarf Curled Scotch (K3) and Red Scarlet (K9) kale seeds (*B. oleracea var. sabellica*) were purchased from West Coast Seeds (https://www.westcoastseeds.com/). Seeds were surface sterilized with incubations in 70% (v/v) ethanol and 30% (v/v) bleach solutions at room temperature beginning with a 4-minute incubation in 3 mL of 70% (v/v) ethanol. The seeds were then rinsed with 3 mL of sterile milli-Q water and 3 mL of 30% (v/v) bleach was added onto each tube for a 7-minute incubation with periodical shaking every 2 minutes. Finally, the bleach solution was removed, and the seeds were rinsed three times with 3 mL of sterile Milli-Q water. Following sterilization, the seeds from each cultivar were plated onto 0.5 x Murashige and Skoog (MS) media plates containing 1% (w/v) sucrose. The seeds were then stratified at 4 °C in total darkness for 96 hours. Following stratification, the kale seedlings were entrained to their respective light treatment for 7 days. To prepare the soil for seedling transplant, ~25 kg of soil (Sun Gro Sunshine Mix #1) was mixed with 8 L of H_2O and then transferred onto 4” square

polypropylene pots. Transplantation occurred once most plants had reached the cotyledon stage at 11 days post-imbibition (dpi).

2.2 Light Conditions

The programmable LED (Perihelion Model) lights used for this experiment were provided by G2V Optics Inc. and were installed inside ventilated growth chambers lined with reflective mylar. The kale plants were grown under a 12-hour light and 12-hour dark regiment. Three different light intensities were tested: 75, 125, 175 PPFD ($\mu mol.m^{-2}.s^{-1}$) (**Supp Figure 1A**). Spectral light conditions were assigned in spectral ratios of R/B and R/FR of low R/B or R/FR, balanced R/B or R/FR and high R/B or R/FR (**Supp Figure 1B**).

2.3 Measurement of Kale Photosynthetic Performance via MultisynQ

Photosynthetic performance was measured following the Photosynthesis RIDES 2.0 protocol using a MultispeQ v1.0 (PhotosynQ LLC, USA)[22]. At mid-day (zeitgeber; ZT6) 34 dpi, the photosynthetic performance of the kale plants was measured by clamping the second true leaf between the MultisynQ sensors ensuring full coverage. The leaf remained in the chamber until the data collection process was completed (~10 s). A total of 10 randomly selected plants were analyzed for each cultivar and light condition.

2.4 Phenotyping measurements

Plants were grown in separate chambers under different light intensity and spectral conditions (**Supp Figure 1**). Each chamber was equipped with single-board Raspberry Pi 3 B+ computers and ArduCam Noir Cameras (OV5647 1080p) with a motorized IR-CUT filter and two infrared LEDs. Pictures of plants were taken every 5 minutes. Plant surface area analysis across light conditions was performed by averaging the area of each plant measured during a 1-hour period (between ZT6 and ZT7) at 22 dpi. Plant surface areas were extracted using Python scripts from the open-source software package PlantCV (https://plantcv.readthedocs.io/), following the methodology described by Gehan *et al*., 2017[23].

2.5 Harvesting and Sample Processing

At 35 dpi, kale leaves were harvested at two time points: end-of-night (ZT23) and end-of-day (ZT11). This was done to capture the expansive metabolic changes occurring during the transitions between night-to-day and day-to-night, respectively. Leaves from three kale plants of the same cultivar were pooled into a labelled 50 mL conical tube and promptly frozen in liquid nitrogen to preserve the proteins and metabolites present. In total, four tubes were collected

from each cultivar per chamber during harvest. Two metal beads were then introduced into each conical tube and the samples were ground by subjecting them to 3x – 30 s/1200 rpm using a Geno/Grinder® - Automated Tissue Homogenizer and Cell Lyser. 100 mg (±1 mg) of each finely-ground sample was then portioned into each of two separate 2 mL Eppendorf Safe-Lock tubes for further processing.

2.6 Anthocyanin Extraction and Quantification:

Anthocyanin analysis was performed as previously described by Neff and Chory (1998), with the following modifications. Specifically, 500 µL of 100% (v/v) methanol-1% (v/v) hydrochloric acid was added to each tube containing the finely ground samples and incubated at 4 °C for 24 hours in darkness. From there, 200 µL of H_2O and 500 µL of chloroform were added and the tubes were centrifuged at 18,000 x g for 5 minutes at room temperature. 400 µL of the supernatant was then transferred over to new tubes and adjusted to a total volume of 800 µL with 60% (v/v) methanol-1% (v/v) hydrochloric acid. A total of 200 µL from each volume-corrected sample was transferred into a well in a 96-well plate and absorbance at 530 nm and 657 nm was measured with a Tecan Spark® plate reader using 60% (v/v) methanol -1% (v/v) hydrochloric acid as the background. The relative anthocyanin content was then derived mathematically using: $Antho = (Abs_{530} - Abs_{657}) \times 1000 \times powder\ weight\ (mg)^{-1}$.

2.7 Metabolite analysis via Gas Chromatography Mass Spectrometry (GCMS)

2.7.1 Metabolite extraction: A total of 700 µL of ice-cold 100% (v/v) methanol was added to the tubes containing 100 mg of finely ground leaf sample and promptly vortexed for ~20 seconds. Using a thermomixer, these were then incubated for 15 minutes at 70 °C with shaking at 1200 rpm. From there, the tubes were centrifuged at 18,000 rpm for 15 minutes and the supernatants were transferred into new tubes. The pellet was then re-extracted using 700 µL of 50% (v/v) methanol containing Ribitol at 25 µL per sample at 0.4 mg/mL in water and vortexed for ~20 seconds until re-suspended. These tubes were then centrifuged at 14,000 rpm for 10 minutes and 600 µL of the supernatant was combined with the previous supernatant. Finally, 100 µL was transferred into new tubes and dried using a vacuum centrifuge at 1 torr at room temperature for 1.5 - 2 hours.

2.7.2 Gas chromatography mass spectrometry analysis:

The dried samples were derivatized by adding 100 µL of methoxamine hydrochloride into each tube and then incubated at 30 °C at 850 rpm for 1 hour using a Thermomixer F2.0 (Eppendorf).

Subsequently, 50 µL of N,O-bis(trimethylsilyl)trifluoroacetamide (BSTFA) was added to each tube and incubated at 50 °C at 850 rpm for 3 hours using a Thermomixer F2.0 (Eppendorf). A total of 150 µL of each sample was then transferred to vials in preparation for injection in the GC-MS. Samples were analyzed via a 7890A gas chromatograph (Agilent) paired to a 5975C quadrupole mass detector (Aglient). The initial GC oven temperature was set at 70 °C and then increased to 325 °C at 7 °C per minute two minutes post-injection where the temperature was then maintained at 325 °C for 3.6 minutes. The injection and ion source temperatures were set to 300 °C and 230 °C, respectively with a solvent delay of 5 minutes. The helium flow rate was also adjusted to a rate of 1 mL/minute. Measurements were performed with electron impact ionization (70 eV) in full scan mode (m/z 33-600). Identification of metabolites was performed based on their mass spectral and retention time index, and how closely they matched to those acquired from the National Institute of Standards and Technology library and the Golm Metabolome Database.

2.8 *Protein extraction and LC-MS analysis*

2.8.1 Protein extraction and LC-MS data acquisition

Kale leaf tissue harvested at ZT23 and ZT11 was flash-frozen in liquid N_2. Tissue was ground in liquid N_2 using a mortar and pestle and aliquoted into 400 mg samples (n=4 replicates). Samples were extracted with 50 mM HEPES-KOH pH 8.0, 50 mM NaCl, and 4% (w/v) SDS at a ratio of 1:2 (w/v). Next, samples were vortexed followed by incubation for 15 min at 95 °C using a Thermomixer F2.0 (Eppendorf) shaking at 1,100 rpm. Samples were subsequently incubated at room temperature for an additional 15 min of shaking followed by clarification at 20,000 x g for 5 min at room temperature, where the supernatant was then retained in fresh Eppendorf microtubes. Protein concentration was estimated by bicinchoninic (BCA) assay (23225; Thermo Scientific), followed by sample reduction using 10 mM dithiothreitol (DTT) for 5 min at 95 °C. Following cooling to room temperature, samples were alkylated using 30 mM iodoacetamide (IA) in dark for 30 min at room temperature without shaking. The alkylation was stopped by addition of 10 mM DTT, followed by a brief vortex and 10 min room temperature incubation without shaking. Samples were digested overnight with 1:100 sequencing grade trypsin (V5113; Promega), followed by quantification of the generated peptide pools using a Nanodrop (Thermo Scientific). Subsequently, samples were acidified with formic acid to a final concentration of 5% (v/v) followed by drying by vacuum centrifugation. Peptide desalting was then performed using ZipTip C18 pipette tips (ZTC18S960; Millipore), with peptides subsequently dried and dissolved in 3% (v/v) ACN / 0.1% (v/v) FA prior to MS analysis. A Fusion Lumos Tribrid Orbitrap mass

spectrometer (Thermo Scientific) was used to analyse the digested peptides in data independent acquisition (DIA) mode using the BoxCarDIA method as previously described[24]. 1 µg of dissolved peptide was injected using an Easy-nLC 1200 system (LC140; ThermoScientific) and a 50 cm Easy-Spray PepMap C18 column (ES903; ThermoScientific). Liquid chromatography and BoxCarDIA acquisition was performed as previously described[24].

2.8.2 Proteomic Data Analysis

All acquired BoxCarDIA data was analyzed using a library-free approach in Spectronaut v14 (Biognosys AG) under default settings. The *B. oleracea* var. *oleracea* proteome (Uniprot:https://www.uniprot.org/ containing 58,545 proteins) was used for data searching. Default search parameters were used for proteome quantification including: a protein, peptide and PSM FDR of 1%, trypsin digestion with 1 missed cleavage, fixed modification including carbamidomethylation of cysteine residues and variable modification including methionine oxidation. Data was Log2 transformed and median normalized with significantly changing differentially abundant proteins determined and corrected for multiple comparisons (Bonferroni-corrected p-value <0.05; q-value).

2.9 *Bioinformatics*

Gene Ontology (GO) enrichment analysis was performed using the Database for Annotation, Visualization and Integrated Discovery (DAVID; v 6.8; https://david.ncifcrf.gov/home.jsp).A) using a significance threshold of p-value < 0.01. Conversion of *B. oleracea* gene identifiers to Arabidopsis was performed using Uniprot (https://www.uniprot.org/) followed by Ensembl Biomart (https://plants.ensembl.org/biomart) for STRING association network analysis and metabolic pathway analysis. STRING association network analysis was performed using Cytoscape v3.10.1 (https://cytoscape.org) in combination with the String DB plugin stringApp and an edge threshold of 0.95. Visualization of GO dotplot was performed using R version 4.3.1 and *ggplot2* package. Metabolic pathway enrichment was performed using the Plant Metabolic Network (PMN; https://plantcyc.org) with enrichment determined using a Fisher's exact test (p-value < 0.01). Final figures were assembled using Affinity Designer (v.2.4.1).

3 Results

3.1 Kale morphology under modified light intensity and spectral composition

To test the effects of light intensity and spectral composition, kale seedlings were grown under three different light intensities: 75 PPFD, 125 PPFD and 175 PPFD (**Supp Figure 1A**), while light spectra experimentation consisted of changes in the ratio of red to blue (R/B) (**Supp Figure 1B**) and red to far-red (R/FR) light (**Supp Figure 1B)**. We found a significant correlation between plant size and increasing light intensity (**Figure 1A-B**), with both K3 and K9 exhibiting an increase in size as a function of the light intensity increasing from 75 PPFD to 125 PPFD **(Figure 1B**). We also found that fresh weight changes ranged from 2.5 to 7.5 g (a 3-fold increase) 35 dpi (**Figure 1B**). Consistent with this, there was also an increase in plant area that correlated with increasing light intensity for both cultivars (**Figure 1B**). Next, we examined the effect of light intensity on diel leaf anthocyanin content, as anthocyanins provide coloration to plants to attract pollinators, as well as acting as antioxidants, which can be beneficial for human health[25,26]. As expected, anthocyanin was not detected in K3, however, there was not a significant difference in anthocyanin content with increasing light intensity in K9, which is known to produce anthocyanins (**Figure 1B**). It is possible that lower intensity than would otherwise be experienced in outdoor growing conditions, the stage of growth and/or a general low stress growth environment resulted in lower anthocyanin production than would be expected.

Next, we tested the effects of light spectral changes (**Figure 1C-D**), while maintaining light intensity under constant 125 PPFD. Here, we found that light differentially modifies the morphology of K3 plants (**Figure 1C**). R/B spectral variation affected K3 fresh weight (**Figure 1D**), with no corresponding change in surface area (**Figure 1D**). Conversely, K9 did not exhibit spectral-dependent weight differences (**Figure 1D**), but did have increasing plant surface area with changes in R/B and R/FR ratios (**Figure 1D**), indicating that red light is particularly important for K9 growth. Despite anthocyanin content below detection level in K3, we do observe significant diel spectral composition differences in K9 (**Figure 1D**). As R/B ratio increases, we find anthocyanins decrease, while we alternatively find that red light (high R/FR ratio) stimulates anthocyanin production over FR (low R/FR ratio). Therefore, changing light intensity and spectral composition impacts morphological characteristics and anthocyanin levels in kale.

3.2 Kale photosynthetic performance with changing light intensity and quality

Next, using a MultispeQ device, we measured a suite of photosynthetic parameters alongside relative chlorophyll levels. These included fluorescence-based parameters such as ΦPSII, ΦNPQ, ΦNO, and Linear Electron Flow (LEF). ΦPSII, or realized steady-state efficiency, which measures how much of the light energy is absorbed by PSII (photosystem II). In other words,

ΦPSII represents the number of electrons transported via PSII per quantum absorbed by PSII[27]. ΦNPQ (non-photochemical quenching) represents the proportion of absorbed light energy that is dissipated as heat, a process that helps protect the plant from excess energy that would otherwise damage PSII[28], while ΦNO (non-regulatory energy dissipation) represents energy that is neither used for photochemistry nor dissipated via regulatory quenching[28]. The other parameters measured were the proton conductivity (gH^+), the electrochromic gradient across the thylakoid membrane (ECSt) and the proton flux (vH^+) which are parameters linked to the ATP synthase efficiency[22].

For the light intensity experiments (**Figure 2A**), an increase in PPFD influenced the chlorophyll content (SPAD) in both K3 and K9. LEF also increased as a function of the light intensity for both K3 and K9 (**Supp Figure 2A**). For K3, we observe a slight increase in proton conductivity (gH^+) and decrease of the electrochromic shift decay across the thylakoid membrane (ECSt) (**Supp Figure 2A**), indicating an increase in conductance[29]. LEF (Linear electron flow) and gH+ are linked to the flow of electrons from PSI to PSII and the flow of protons through the ATP synthase[22], which supports the observed increase in plant fresh weight and area as the plant produces more ATP required for plant growth. For the K9 cultivar, ΦPSII seemed to reach a plateau under 125 PPFD (**Figure 2A**), with ATP synthase parameters demonstrating limited light intensity-induced changes.

However, when light spectral composition was modified (**Figure 2B**), both K3 and K9 exhibited a decrease in SPAD and ΦPSII with increasing R/B. Conversely, SPAD and ΦPSII increased as R/FR increased for both cultivars. No change in the ATP synthase related parameters were observed for K3 or K9, except LEF, which increased with increasing R/B (**Supp Figure 2B**). Thus, kale photosynthetic parameters and chlorophyll content can be modulated by changes in light intensity and spectral composition.

3.3 Assessing changes in kale metabolic content with varied light intensity and spectral composition

To uncover a potential molecular rationale for the observable phenotypic changes, we next analyzed the metabolite content of each cultivar by GC-MS when grown under the different light intensities (**Figure 3**), R/B ratios (**Figure 4**) and R/FR ratios (**Figure 5**). Amino acids (15), fatty acids (3), organic acids (11), polyamines (2), sterols (2), sugars (5), and sugar alcohols (2) were detected and quantified. Under differing light intensities, we observed cultivar and light intensity specific differences for Asn, Asp, Glu, Lys, Pro, Ser, Gly, and Ile. Asp, Glu and Pro that

correlated with an increase in light intensity in both cultivars and was more noticeable at ZT23 compared to ZT11. Another noticeable trend was a peak in Asn, Gly, Ile, Lys and Ser at both time-points under 125 PPFD. Conversely, change in R/B ratio (**Figure 4**) resulted in several amino acids having changes at ZT11. In particular, Gly which increased with increasing red light at ZT11 in both cultivars. Other changes seemed cultivar and time of day specific, such as Asn, which increased in K3 at ZT11 under high R/B, or Asp, which increased in K9 at ZT11 under high R/B. Alternatively, our main observations with modified R/FR included an increase in Ala, Asn and Lys levels in K3 and K9 at both time-points under balanced R/FR. We also find GABA and Gln quantities to be highest at ZT11 under balanced R/FR in both cultivars.

In the organic acids and polyamines, chlorogenic acid (related to the phenylpropanoid pathway, which includes lignin, flavonoids, coumarins, and lignans), glyceric acid, succinic acid, 3-O-coumaroyl-quinic acid and quininic acid were all positively affected by increasing light intensity (**Figure 3**). Additionally, citric acid and malic acid showed a large increase in both K3 and K9 under 175 PPFD, with malic acid higher at ZT11 and citric acid higher at ZT23 (**Figure 3**). With citric acid linked to plant growth and photosynthesis by alleviating plant stress[30], this may indicate that 175 PPFD represents a light intensity that initiates stress in kale. For our spectra experiments, increases quininic acid at ZT23 and citric acid, succinic acid, malic acid, and glyceric acid at both ZT11 and ZT23 were found with increasing R/B in both K3 and K9 (**Figure 4**), however, glyceric acid only increased at ZT23 in K9. We also found Spermidine, a polyamine, to be lower in K9 at ZT23 under balanced R/B (**Figure 4**). As well, Chlorogenic acid, which is important for anthocyanin production, was higher in K9, compared to K3, likely aligning with its known purpling phenotype (**Figure 5**). Lastly, with increasing R/FR, we find that K9 exhibits a greater overall number of organic acid / sterol compounds changing in abundance compared to K3 (**Figure 5**), except for quininic acid and 3-O-coumaroyl-D-quinic acid (**Supp Figure 3-5**).

With links to plant stress response, auxin perception and cell wall biosynthesis[31], the sugar alcohol Myo-inositol increases as a function of light intensity in both cultivars at ZT11 (**Figure 3**). We find Myo-inositol in K3 to be more affected by high PPFD than K9. However, Myo-inositol was higher in K3 at ZT23 under low R/B relative to K9 and higher at ZT11 in all the conditions relative to K9 (**Figure 4**). Glycerol decreases at ZT23 when R/B increased (**Figure 4**), which contrasts most changes we observe when R/B increased. Myo-inositol was the only sugar alcohol with a significant change in K3 over K9, which manifested under high R/FR at ZT11 (**Figure 5**).

Among sugar metabolites, fructose and glucose exhibited similar trends, showing a slight increase with light intensity (**Figure3**). Mannose-6-phosphate (M6P) increases with intensity in both cultivars and seems greatly affected in K3 with intensity under 175 PPFD. M6P is associated with protein sorting and transport[32], stress, and the cell wall[33], all of which may contribute to adaptation to higher light intensity[34]. The sugars fructose and glucose increased as R/B increased in K9, while K3 showed no statistically significant changes (**Figure 4**). Interestingly, M6P was higher in K3 at ZT23 under balanced R/B, while it was lower as R/B increased at ZT11 (**Figure 4**). Sucrose showed very little change at either time-point. Finally, trehalose in K9 seemed to increase with the R/B, while K3 only exhibited an increase at ZT11 under high R/B. Amongst the sugars, fructose and glucose was maximal in K3 at ZT23 under balanced R/FR, while in K9, it was largely unchanged. At ZT11, K9 was increased in fructose and glucose under low and balanced R/FR compared to high R/FR. Finally, both M6P and sucrose were higher in K9 under balanced R/FR at ZT23 (**Figure 5**). Collectively, our results indicate that changing light intensity and quality has dramatic impacts on overall plant metabolism in kale.

3.4 Analysis of kale light intensity- and spectra- responsive proteome

We sought to further contextualize the observed phenotypic and metabolite changes by using quantitative proteomics to examine the protein-level changes in K3 and K9 over the varying light intensities and spectral compositions. We were able to quantify a total of 5,493 proteins across our intensity experiments, and 6,527 proteins across spectra experiments (**Supp Table 3**). We next identified significantly changing proteins using a fold-change analysis comparing each varied light intensity or spectra to a control, considering 75 PPFD as control for light intensity compared to 125 PPFD and 175 PPFD (**Figure 6A; Supp Table 3**) and low R/B (**Figure 6B; Supp Table 3**) and low R/FR (**Figure 6C; Supp Table 3**) ratios compared to balanced and high R/B and R/FR ratios, respectively. For our intensity experiments, K3 exhibited the most significantly changing proteins from 75 PPFD to 125 PPFD at ZT11 and from 75 PPFD to 175 PPFD at ZT23. For spectral experiments, K9 appeared more responsive to increasing R/B and R/FR ratios, possessing more significantly changing proteins than K3. Specifically, this involved low to high R/B and R/FR ratios at ZT11, and increases under both balanced and high R/B and R/FR ratios at ZT23.

We next performed gene ontology (GO) enrichment analysis using the significantly changing proteome to resolve what biological processes are responsive to changes in either light intensity or spectral composition (**Figure 6D**). This analysis revealed biological processes related to the

cell wall, photosynthesis / pigment metabolism, oxidative stress, carbohydrate metabolism, and lipid metabolism across both intensity and spectra experiments. With increasing intensity, we observed an enrichment of more biological processes when considering down-regulated versus up-regulated proteins at both ZT23 and ZT11. Alternatively, we increased R/B ratio, we observed more enriched biological processes among up-regulated proteins at both time-points. Finally, with increasing R/FR ratio, we observed more enriched biological processes among up-regulated proteins at ZT23, and among down-regulated proteins at ZT11.

Plant growth is associated with changes in cell wall composition and structure[35]. In accordance with the changes in growth parameters detailed above, we observed changes in the abundance of proteins involved in cell wall processes. In our intensity experiments, we primarily observed the down-regulation of proteins involved in cell wall related biological processes with increasing light intensity at both ZT23 and ZT11. This included the GO terms 'Plant-Type Secondary Cell Wall Biogenesis' (GO:0009834), 'Cell Wall Organization' (GO:0071555) 'Xyloglucan Metabolic Process' (GO:0010411) and 'Cell Wall Biogenesis' (GO:0042546). Xyloglucan is an abundant component of primary cell walls[36]. Among the down-regulated proteins in K3 we find enrichment of 'Pectin Catabolic Processes' (GO:0045490) at ZT11 under 125 PPFD, with pectin representing another major component of plant primary cell walls[37]. With increasing R/B, we also identified an enrichment of the GO term 'Xyloglucan Metabolic Process' among up-regulated proteins in K3 at ZT11. In our R/FR spectral experiments, increasing R/FR down-regulated proteins involved in 'Xyloglucan Metabolic Process', 'Cell Wall Organization', and Cell Wall Biogenesis' in K3 at ZT11 under high R/FR. Conversely, a more complex response was observed at ZT23 in K3, with 'Xyloglucan Metabolic Process and 'Cell Wall Biogenesis' enriched among up-regulated proteins under balanced R/FR, and down-regulated proteins enriched for 'Plant-Type Secondary Cell Wall' and 'Cell Wall Modification' (GO:0042545) at the highest R/FR. Taken together, these results indicate that light conditions substantially impact cell wall related processes in kale.

While the MultiSynQ measurements shed light on alterations in photosynthesis and chlorophyll content with changing light intensity, our GO analysis revealed enrichment of terms associated with photosynthesis and pigment metabolism. In our intensity experiments, down-regulated proteins were enriched for 'Photosynthesis, Light Harvesting in Photosystem I' (GO:0009768) under the highest PPFD in K3 at ZT23. In our R/B spectra experiments, a balanced R/B ratio in K9 seemed to be optimal for photosynthetic performance, with up-regulated proteins enriched for the GO terms 'Photosynthetic Electron Transport in Photosystem I' (GO:0009773) and

‘Photosynthesis, Light Harvesting in Photosystem I’ at ZT11. Additionally, we observed an enrichment of ‘Carotenoid Metabolic Process’ (GO:0016117) among down-regulated proteins at ZT11 in K3 under balanced R/B, and among up-regulated proteins under high R/B in K9 at ZT23. Finally, up-regulated proteins at ZT11 in K9 under high R/FR were enriched for the GO term ‘Photosynthesis’ (GO:0015979). These results suggest that kale photosynthetic processes are impacted by both light intensity and spectra composition, with increasing light intensity generally resulting in a down-regulation of light harvesting proteins and increasing red light ratios in higher photosynthetic processes.

In accordance with our measured changes in the abundance of proteins related to photosynthetic processes, we also observe protein-level changes associated with general metabolic processes, such as carbohydrate metabolism and lipid metabolism. In our intensity experiments, we observed a down-regulation of proteins enriched for ‘Lipid Catabolic Process’ (GO:0016042) and ‘Glycolytic Process’ (GO:0006096) in K3 at ZT11. With increasing R/B light, we observed an increase in proteins related to lipid biosynthesis in K3. This included enriched GO terms ‘Wax Biosynthetic Process’ (GO:0010025), ‘Lipid Transport’ (GO:0006869), and ‘Lipid Biosynthetic Process’ (GO:0008610) at ZT11, and of ‘Lipid Oxidation’ (GO:0034440) at ZT23. ‘Glycolytic Process’ was enriched among down-regulated proteins at ZT11 and ZT23 in K9 under high R/B, but among up-regulated proteins under balanced R/B in K3 at ZT23. Finally, at ZT11 down-regulated proteins were enriched for ‘Carbohydrate Metabolic Process’ (GO:0005975) in K3 under balanced R/B, and at ZT23 in both K3 and K9 there was an enrichment for the GO term ‘Carbohydrate Metabolic Process’ under balanced R/B ratio for up-regulated proteins. In our increasing R/FR experiments, at ZT11 down-regulated K3 proteins were enriched for ‘Fatty Acid Biosynthetic Process’ (GO:0006633), and at ZT23, down-regulated K9 proteins were enriched for ‘Fatty Acid Metabolic Process’ (GO:0006631). Additionally, ‘Lipid Oxidation’ was enriched among up-regulated K3 proteins under balanced R/FR. Glycolysis and TCA cycle proteins appeared to be down-regulated in K3 at both ZT11 and ZT23 under balanced R/FR, with enrichment of ‘Succinyl-CoA Metabolic Process’ (GO:0006104) and ‘Glycolytic Process’ at ZT11 and ‘Mitochondrial Respiratory Chain Complex I Assembly’ (GO:0032981), along with ‘Glycolytic Process’ at ZT23 in K9. Finally, ‘Carbohydrate Metabolism’ was enriched amongst down-regulated proteins in K9 at ZT11 under balanced R/FR, while ‘Glucan Catabolic Process’ (GO:0009251) was enriched amongst up-regulated under high R/FR in K9 at ZT11. Thus, light intensity and spectral composition play a large role in protein levels associated with metabolic processes in kale.

High light intensity can be associated with oxidative stress, and we observed changes in proteins associated with oxidative stress responses in our intensity and spectra experiments. For instance, in our intensity experiments, both kale cultivars had up-regulated proteins at ZT11 showing enrichment for 'Superoxide Metabolic Process' (GO:0006801) under 175 PPFD. Interestingly, under 175 PPFD, the K3 cultivar showed an enrichment of the terms 'Toxin Catabolic Process' (GO:0009407), 'Response to Oxidative Stress' (GO:0006979), and 'Glutathione Metabolic Process' (GO:0006749) amongst down-regulated proteins at ZT23, indicating some diel regulation and cultivar-specific oxidative responses. We additionally observed potential cultivar-specific oxidative stress response in our R/B spectral experiments at ZT11, with K3 down-regulated proteins enriched for 'Glutathione Metabolic Process' under high R/B and K9 up-regulated proteins enriched for 'Hydrogen Peroxide Catabolic Process' (GO:0042744) under high R/B. At ZT23, only K3 showed altered oxidative stress response, with down-regulated proteins enriched for 'Superoxide Metabolic Process' under high R/B and up-regulated proteins enriched for 'Toxin Catabolic Process' and 'Glutathione Metabolic Process' under high R/B. In our R/FR spectral experiments, K3 up-regulated proteins were enriched for the terms 'Toxin Catabolic Process' and 'Glutathione Metabolic Process' under high R/FR at ZT11, while K9 down-regulated proteins were enriched for 'Response to Oxidative Stress' under balanced R/FR. At ZT23, K3 down-regulated proteins were similarly enriched for 'Response to Oxygen-Containing Compound' (GO:19011700) and 'Response to Hydrogen Peroxide' (GO:0042542), while up-regulated proteins were enriched for 'Glutathione Metabolic Process', under balanced R/FR. Overall, these results indicate diel regulated, cultivar-specific responses to oxidative stress with altered red light intensity and quality.

To further contextualize our GO analysis results, we performed an association network analysis using STRING-DB (https://string-db.org/) for each of the Intensity, R/B and R/FR spectra experimental conditions in order to further contextualize proteome-level responses (**Figures 7-8**). As *Arabidopsis thaliana* (Arabidopsis) has more bioinformatic resources, we first converted the *B. oleracea* gene identifiers for all quantified proteins in the study to Arabidopsis gene identifiers (AGI) using UniProt (https://www.uniprot.org/) and Ensembl Biomart (https://plants.ensembl.org/biomart). We identified unique AGIs for 90% of the significantly changing proteins in our intensity experiments (2395/2662), along with 88.9% (2222/2499) and 89.4% (2520/2819) in our R/B and R/FR spectra experiments; respectively. Using a highly stringent STRING-DB edge score of 0.95, this analysis corroborated our phenotyping experiments and GO analysis. For photosynthesis and pigment metabolism, we observed a down-regulation of protein with increasing intensity and R/FR, but an up-regulation with

increasing R/B ratio. Regarding oxidative stress responses, we observed complex changes in detoxification, glutathione metabolism and ascorbate metabolism, with proteins both up- and down-regulated across both intensity and spectra experiments. We additionally observe hubs of changing proteins related to carbohydrate metabolism, fatty acid biosynthesis and degradation, glycolysis and TCA cycle that align with our GO enrichment findings. In addition to our GO enrichment analysis, the association network analysis uniquely revealed large hubs of differentially expressed proteins related to spliceosome, ubiquitin / proteasome and phenylpropanoid metabolism.

Finally, using the Arabidopsis gene identifiers for the significantly changing proteins with increasing intensity, R/FR and R/B, we performed metabolic pathway enrichment using the Plant Metabolic Network (PMN; https://plantcyc.org; **Supp Tables 4-6**). The enriched pathways corroborated our findings with metabolite analysis, GO analysis and association networks, with enriched pathways being resolved for amino acid metabolism, lipid metabolism, carbohydrate metabolism, oxidative stress response, glucosinolate production, general metabolic processes, growth-associated hormones, photosynthesis and pigment metabolism (chlorophyll and carotenoids).

4 Discussion

Light intensity and spectral composition are major determinants of plant growth, metabolite content and yield. Given the health benefits of kale and its increased usage in vertical farm settings, it is important to understand how exposure to different light intensities and R/B or R/FR spectral compositions impact growth and nutritional quality. Several studies have identified changes in growth, yield and metabolite content in *Brassica* microgreens under different light intensities[38,39], and under different spectral compositions[16–18], however, there is a notable lack of knowledge about their effects at the molecular level, which is critical for future breeding endeavors to yeild gains. As a result, our combined use of plant phenotyping, physiology, metabolomics and quantitative proteomics offers a comprehensive analysis of the effects of varying light intensity and quality on two closely-related kale cultivars. Overall, our results point to changes in shade avoidance response, with shade presenting as lower light intensity, low blue light and low R/FR ratios[40], and manifesting as changes in growth and development, photosynthesis, phenylpropanoid metabolism, cell wall processes, amino acid production, carbohydrate metabolism, lipid and fatty acid metabolism and organic acid production. We further contrast the phenotypic, physiological and molecular responses of two kale cultivars with time-of-day precision, offering new levels of insight for precision vertical farming.

4.1 *Photoreceptors*

Changes in light quality are detected by plant photoreceptors, which invoke signal transduction pathways that impact plant growth and development. These photoreceptors include phytochromes (PhyA-E), which sense R/FR light, cryptochromes (CRY1-3) and phototropins (PHOT1/2), which sense blue light, and UVR8, which senses UV-B[41]. We quantified several of these in our experiments, including PhyB (A0A0D3BBQ1), CRY1 (A0A0D3E8M6), PHOT1 (A0A0D3BGL7; A0A0D3BGL8), PHOT2 (A0A0D3ECB2), and UVR8 (A0A0D3E235). However, only a few of them showed significant changes in abundance across a few conditions. These photoreceptors typically undergo regulation by phosphorylation[42–47]; thus, it is likely post-translational modifications, rather than simply protein abundance that govern their responses to changes in light intensity and spectral composition.

4.2 Proteome changes with changing light intensity and quality are associated with changes in shade avoidance responses

4.2.1 Growth, development and hormone signaling

Previous studies have reported a linear relationship between light intensity and fresh weight in pea microgreens[48], as well as kale, cabbage, arugula and mustard[49], similar to our observations. Importantly, several of these studies used PPFD up to 600 $\mu mol \cdot m^{-2} \cdot s^{-1}$ with increases in fresh weight at the upper PPFD values, suggesting our highest light intensity of 175 PPFD is not inducing a high light stress response. As light intensities used in vertical farming are typically lower, around 200 PPFD[50], our study is highly relevant to informing practices for kale grown in vertical farms. With our spectra experiments, we only observed an increase in K3 fresh weight with increasing R/B ratio, and an increase in K9 surface area with both increasing R/B and R/FR ratios. In alignment with this, a previous report found an increase in dry mass and seedling area specifically with red kale varieties, whereas blue light had a stronger effect on green kale dry mass[51], suggesting growth parameters under different light qualities are cultivar-dependent. This emphasizes the need to generate cultivar-specific molecular response data, such as that generated here, to uncover unique breeding opportunities.

Our proteomic data revealed that under the conditions tested, hormone pathways associated with plant growth and development, including brassinosteroids (BR) and auxin, play a key role. For example, we observed down-regulation of K3 proteins involved in BR signaling with increasing light intensity. This is consistent with previous reports of Arabidopsis BR biosynthetic genes *CONSTITUTIVE PHOTOMORPHIC DWARF* (*CPD)*, and *DWF4* being dark

induced, but light repressed[52–55], as well as the transcription of BR signaling proteins *bri1 EMS SUPPRESSOR1 (BES1)* and *BRASSINOZOLE RESISTANT1* (*BZR1)* elevation at night and repression during the day[54]. Additionally, BR signaling appears to play a role in shade avoidance response[56,57]. In our study, we observe the down-regulation of kale DIMUNUTO (DIM)/DWF1 protein (A0A0D3CI99) in K9 with increasing light intensity, which has been reported to be involved in shade-induced hypocotyl elongation in Arabidopsis[58]. We additionally observe down-regulation of BZR1 (A0A0D3CWJ3) in K9 at ZT11 and up-regulation at ZT23 with increasing light intensity, suggesting differential regulation of its protein stability and abundance. The observed down-regulation within our dataset with increasing light intensity indicates relief from perceived shade conditions. In addition to BR signaling proteins changing with light intensity, we observed an up-regulation of proteins involved in auxin signaling with an increasing R/B ratio in K3. Previous work has identified red light as inducing auxin flux from leaves to roots, possibly through increased abundance of *PINOID1* (*PIN)1, PIN3,* and *PIN4*[59], thus our observed up-regulation of PIN3 (A0A0D3CZR1) in K3 under high R/B may indicate a similar response. Additionally, up-regulation of auxin signaling is consistent with increased shade avoidance response, where auxin signaling has been shown to play a role in the hypocotyl elongation[60]. Overall, our results indicate that modulation of light intensity and spectral quality induce changes in kale growth and development, possibly through changes in key hormone signaling pathways.

4.2.2 Cell wall

Our observation of down-regulated BR biosynthesis and signaling proteins under increasing light intensity suggests a down-regulation of shade avoidance responses. Related to BR shade avoidance response is changes in cell wall structure, particularly by the action of xyloglucan endotransglucosylase/hydrolases (XTHs) and expansins[61,62], with cell wall modification promoting elongation of the hypocotyl to drive growth toward light. Within our dataset, we observe a multitude of cell wall proteins changing in abundance in response to light intensity and spectral composition, potentially relieving shade-like conditions in both kale cultivars. Specifically, we note a down-regulation of cell wall organization proteins, primarily XTHs, expansins (EXPAs), and pectinesterases (PMEs) with increasing light intensity and R/FR ratio, but an up-regulation of XTHs with increasing R/B, consistent with changes in the plant perception of shade. Interestingly, more members of the XTH family were down-regulated in K9 with increasing light intensity and K3 with increasing R/FR, suggesting K9 may be more

sensitive to changes in intensity and K3 more sensitive to changes in red light wavelengths. This is also consistent with our growth observations.

4.2.3 Photosynthesis

Light intensity and quality also critically impact plant photosynthesis and light harvesting, as well as pigment metabolism (e.g. chlorophyll and carotenoids). Our LEF measure, used as an approximation for photosynthetic rate[22], indicates a higher photosynthetic rate with increasing intensity and R/B ratio in both K3 and K9, and with increasing R/FR in K9. Intriguingly, our proteomics data implies a concurrent down-regulation of light harvesting proteins at higher intensities at ZT23 in K3, with LHCA1 (A0A0D3CTW2; A0A0D3DT59), LHCA2 (A0A0D3DUU9; A0A0D3BWE5), LHCA3 (A0A0D3E520), LHCB2.4 (A0A0D3DBD3), LHCB4.2 (A0A0D3CLT0) and LHCB5 (A0A0D3BQY2) all down-regulated. In the K9 cultivar, we only find LHCA2 and LHCB5 were down-regulated, indicating a stronger response in K3. This is likely due to sufficient, or even excessive light energy under the 175 PPFD light intensity, such that light harvesting potential has been reached, a phenomenon which is well-established in response to light/shade levels[63–65]. Correspondingly, under a higher R/FR ratio we find the down-regulation of light harvesting proteins, consistent with the relief of shade avoidance conditions. By contrast, under a balanced R/B ratio we see an up-regulation of light harvesting and photosynthesis-related proteins, particularly in K9, suggesting an optimal ratio of R/B light is best for light harvesting and photosynthetic responses. Red light can act to promote photosynthesis and plant growth, but excessive amounts of red light can cause an imbalance in PSI and PSII, and thus blue light is needed[66]. Overall, our data suggest light-dependent differences exist between the two cultivars, with K3 light harvesting proteins showing a stronger response to light intensity changes, and K9 more to changes in spectral composition.

4.3 Alteration of light intensity and spectral composition changes kale nutritional profile

Kale consumption is associated with myriad health benefits as a result of anthocyanins and flavonoids, carotenoids, amino acids, glucosinolates, vitamins, sugars and phenolic compounds[18,67,68]). Several studies have assessed the impact of light intensity and quality on nutritional composition in a range of *Brassica* microgreens[38,69], however, none provide data linking phenotypes with metabolic and proteomic profiles with time-of-day precision.

4.3.1 Anthocyanins / phenylpropanoids

Anthocyanins are a natural antioxidant source, beneficial for human health as reactive oxygen species scavangers[70,71] with the generation of anthocyanins typically driven by light[72]. In our study, we were only able to detect anthocyanins within the K9 cultivar, with no significant difference with changing light intensity, but a significant decrease with increasing R/B, and increase with increasing R/FR. Within our metabolite analysis, we observed changes associated with anthocyanin and phenylpropanoid metabolism: including chlorogenic acid and quininic acid with changing R/B, and sinapinic acid, chlorogenic acid, quininic acid and 3-coumaroyl-D-quinic acid in R/FR. Additionally, within our metabolic pathway analysis, we observed significant pathway enrichment associated with phenylpropanoid and flavonoid metabolism with increasing R/B and R/FR composition. As expected with increasing R/FR, we see a significant up-regulation of flavonoid biosynthetic pathways, which is more pronounced in the K9 cultivar and consistent with our ability to detect anthocyanins in this cultivar. Intriguingly, we observe an up-regulation of phenylpropanoid biosynthesis pathways in K9 with increasing R/B at ZT23, which contrasts with our observed anthocyanin levels. It is possible that at ZT23 the phenylpropanoid pathway is diverting the flux toward other phenylpropanoid products. For example, we see the coumarin biosynthesis pathway enriched in our metabolic pathway analysis, coupled with observed up-regulation of DEFECTIVE IN CUTICULAR RIDGES (DCR; A0A0D3DD85), ENHACED PSEUDOMONAS SUSCEPTIBILITY1 (EPS1; A0A0D3D884) and COUMARIN SYNTHASE (COSY; A0A0D3CEC8) in K9 at ZT23, indicating possible increased coumarin biosynthesis[73–75]. Thus, our results suggest the ideal conditions for kale anthocyanin production under lower intensities involves the use of a high R/FR spectral composition, with higher R/B ratios having negative impacts by possibly diverting the phenylpropanoid pathway toward other products.

4.3.2 Glucosinolates

Another component of kale consumption beneficial for human health is that of glucosinolates, which are amino acid-derived with sulphur and thioglucosidic moieties[76,77]. Playing a role in kale flavour and plant defense, glucosinolates can also act as anticancer compounds for human health[78]. Our proteomic analyses indicated changes in glucosinolate metabolism with increasing light intensity and R/B ratio. In our intensity experiments, the K9 cultivar showed a down-regulation of proteins associated with glucosinolate catabolism as light intensity increased. Our metabolic pathway analysis indicated increased biosynthesis of glucosinolates in K3, thus the cultivars might achieve the same elevated levels of glucosinolates at higher light intensities through differing mechanisms. In our assessment of R/B responses, we observe a decrease in

glucosinolate catabolism by GO analysis and an increase in glucosinolate biosynthesis by metabolic pathway analysis in K3. This has previously been observed with levels of the glucosinolates sinigrin, glucobrassicin, and 4-methoxy glucobrassicin in *B. napus* sprouts exposed to increasing red light levels[79], while another study found differential cultivar responses with changing light intensities in Chinese cabbage[80].

4.3.3 Carotenoids

In addition to flavonoids and glucosinolates, carotenoids are also antioxidants compounds beneficial to human health[81]. Within our proteomic data, we find K3 has lower carotenoid production with increasing light intensity, combined with decreasing protein abundance of CAROTENE CIS-TRANS-ISOMERASE (CRTISO; A0A0D3DYP6), 15-CIS-PHYTOENE DESATURASE (PDS; A0A0D3BJ64) and PHYTOENE SYNTHASE1 (PSY1; A0A0D3AJG7). In our spectral experiments, it appears that increasing red light in both the R/B and R/FR experiments drives increased carotenoid biosynthesis in the K9 cultivar, along with increasing protein abundance of CRTISO (A0A0D3DYP6), LYCOPENE EPSILON CYCLASE2 (LUT2; A0A0D3B320), PSY1 and PDS in R/B experiments and PDS, CRTISO and CYP97B3 under R/FR conditions. These results suggest that K3 might be more sensitive to light intensity changes and K9 to levels of red light. We thought it interesting to find lower carotenoid biosynthesis with increasing light intensity in K3 as carotenoids tend to increase with higher light intensity[82], however there is evidence in pepper of lower carotenoids with increasing light intensity that is suggested to be due to a higher photo-oxidation rate than that of carotenoid synthesis[83,84].

4.3.4 Amino acids

Our metabolite profiling identified several changes in the amino acid content of K3 and K9 kale in response to changing light intensity and quality. We observe extensive changes in our metabolic and proteomic analyses associated with the glutamate family of amino acids, including glutamine, glutamate, GABA, proline, arginine. These amino acids represent the highest amino acid quantities in plants, with glutamic acid and proline present at the highest quantity in kale[85]. Glutamate metabolism also represents a critical link between nitrogen and carbon metabolism through the TCA cycle, with several glutamate catabolism products, including proline and GABA, associated with plant stress responses[86,87]. With increasing light intensity, we observe a down-regulation of proteins involved in glutamate catabolism, including GLUTAMATE DEHYDROGENASE1 (GDH1; A0A0D3EEJ0) and GDH2 (A0A0D3AI31), which

converts glutamate to glutamine, DELTA-1-PYRROLINE-5-CARBOXYLATE SYNTHASE B (P5CSB; A0A0D3BXP3), involved in proline biosynthesis, N-ACETYLGLUTAMATE SYNTHASE (NAGS; A0A0D3A172) and N-ACETYLGLUTAMATE KINASE (NAGK; AT3G57560), which are steps toward ornithine biosynthesis, and CARBAMOYL-PHOSPHATE SYNTHASE ALPHA (CARA; A0A0D3CZA9), toward arginine biosynthesis. We found this trend in both K3 and K9 and at both ZT11 and ZT23, suggesting increasing the light intensity in our experiments may relieve stress responses associated with low light. This also coincides with increased glutamic acid accumulation at higher light intensities (**Figure 3**). However, we also observe an increase in proline in our metabolomics data under higher light intensities, with a significant increase in K3 at ZT11, which may suggest sufficient levels of proline and the down-regulation of P5CSB to prevent further accumulation. Similar findings are present in our proteome data from increasing R/B ratio, with proteins associated with proline biosynthesis and glutamate metabolism primarily down-regulated at ZT23 in both K3 and K9. However, although we did not find a significant difference in the levels of glutamic acid or proline in either cultivar. Thus, increasing amounts of red light in the presence of blue light may be associated with less stressful conditions, however not to the extent of our light intensity manipulation. The situation was slightly more complex with increasing R/FR light. Our finding of P5CSA up-regulation suggests increased proline biosynthesis, while increase in ARGINASE 1 (ARGAH1; A0A0D3B8E0) and CARA, suggest enhanced flux through the glutamate pathway in K3, whereas glutamate metabolic proteins are down-regulated in K9. The metabolite data displayed a peak at balanced R/FR in K3 for the amino acids glutamate, glutamine and GABA, but a less clear trend in K9, suggesting differential amino acid regulation between the cultivars with changing R/FR light ratios.

The aspartate-derived amino acids are also of great importance for human nutrition as they cannot be synthesized by the human body and must be obtained through diet[88]. This includes the essential amino acids lysine, threonine, methionine and isoleucine. Of particular interest is lysine, as it is generally of very low abundance in plants[89]. We observe a general down-regulation of proteins associated with lysine biosynthesis as light intensity increases, particularly in K3 at ZT11, with a down-regulation of ASPARTATE KINASE (AK2) and of DIHYDRODIPICOLINATE SYNTHASE1 (DHDPS1), both involved in lysine biosynthesis. However, within our metabolite data, there is a significantly higher amount of lysine present in K3 under 125 PPFD than either 75 or 175 PPFD, suggesting more complex regulation of lysine biosynthesis. This has previously been observed in attempts to engineer greater lysine production, where lysine has been shown to allosterically inhibit the activity of DHDPS1[90], as well as impacting other aspartate-derived amino acids, such as threonine[91]. In contrast to

increasing light intensity, increasing R/B ratio induced an up-regulation of proteins involved in lysine biosynthesis, which only somewhat mirrored an increase in lysine metabolite abundance at ZT11. Finally, proteomic data suggested an increase in R/FR ratio leads to an up-regulation of lysine biosynthesis in K9, which along with the increasing R/B trend suggests greater proportion of red light may promote lysine synthesis, whereas balanced R/FR seems to have the highest measurable lysine levels.

We previously identified diel regulation of branched-chain amino acids (BCAA) in kale[21], of which we observed changes in the levels of isoleucine with intensity (highest under 125 PPFD), which mirrored down-regulation of branched chain amino acids catabolic enzymes in our proteomic data. Additionally, valine trending higher under balanced R/FR, mirrored the down-regulation of valine catabolic enzymes in our proteomic data under balanced R/FR. Finally, we observe altered serine levels correlating with changing light intensity and spectral composition. Given serine is a key substrate for other essential amino acids, such as methionine and cysteine[92], this is likely of interest for human nutrition.

4.3.5 Carbohydrates

Aligning with our observed changes in amino acids and corresponding metabolic enzymes, we also observe changes in carbohydrate metabolism, manifesting in the differential abundance of sugars and of enzymes involved in carbohydrate metabolism. In our proteomic data, we observe a general down-regulation of proteins involved in glycolysis and starch degradation, as well as trehalose biosynthetic proteins. As trehalose has been associated with shade avoidance[93] and regulation of the circadian clock[94], this is consistent with reduced stress under low light intensities associated with shade as we increase the light intensity from 75 PPFD to 125 and 175 PPFD. Specifically, we find that increasing the R/B ratio down-regulates proteins associated with glycolysis in both cultivars, and mannose metabolism in K9. This was consistent with the lowest M6P levels found in K9 under balanced R/B. Finally, increasing R/FR was associated with the down-regulation of glycolytic proteins in both cultivars, as well as myo-inositol biosynthetic proteins in K9. Conversely, myo-inositol biosynthesis was up-regulated in K3 with increasing R/FR. In K3, this showed moderate correlation with corresponding metabolite levels, as myo-inositol level was significantly higher in K3 at ZT11 under high R/FR. As myo-inositol is involved in many biological processes, including auxin biosynthesis, membrane biogenesis, light and abiotic stress responses[95], its modulation may impact several of the morphological responses we observe.

4.4 Conclusions

In summary, we present an integrated systems-level analysis of two closely-related kale cultivars under increasing light intensity, R/B and R/FR spectral ratios with time-of-day precision. Our data reveals that light intensity and spectral composition can modulate myriad processes within kale, including changes in photosynthesis, cell wall, nutritional components such as amino acids, carbohydrates, phenylpropanoid metabolism among others. Overall, this rich dataset serves not only as a fundamentally interesting dataset for further characterization of kale, it also offers to inform future opportunities for enhanced kale cultivation in vertical farms for desired morphological and nutritional traits.

ACKNOWLEDGEMENTS

The authors thank the Natural Sciences and Engineering Research Council of Canada (NSERC), Alberta Innovates (AI) and Canada Foundation for Innovation (CFI) for funding. The authors thank G2V Optics Inc. for providing their programmable LED lighting system as well as Jack Moore of the Alberta Proteomics and Mass Spectrometry Facility for assistance with mass spectrometer operation and maintenance.

AUTHOR CONTRIBUTIONS

R.G.U. and S.S. conceptualized the study. S.S., B.C., L.I., C.K., N.B. performed research and data acquisition. S.S., L.E.G. and R.G.U. analyzed the data and wrote the paper with input from all authors.

DATA AVAILABILITY

All raw data files have been uploaded to ProteomeXchange (http://www.proteomexchange.org/) via the PRoteomics IDEntification Database (PRIDE; https://www.ebi.ac.uk/pride/) with the dataset identifier PXD055752.

CONFLICTS OF INTEREST

None to declare

REFERENCES

1. Satheesh, N. & Workneh Fanta, S. Kale: Review on nutritional composition, bio-active compounds, anti-nutritional factors, health beneficial properties and value-added products. *Cogent Food Agric.* **6**, 1811048 (2020).
2. Kim, S. Y., Yoon, S., Kwon, S. M., Park, K. S. & Lee-kim, Y. C. Kale juice improves coronary artery disease risk factors in hypercholesterolemic men. *Biomed. Environ. Sci.* **21**, 91–97 (2008).
3. Raychaudhuri, S., Fan, S., Kraus, O., Shahinozzaman, M. & Obanda, D. N. Kale supplementation during high fat feeding improves metabolic health in a mouse model of obesity and insulin resistance. *PLOS ONE* **16**, e0256348 (2021).
4. Rachwał, K. *et al.* Red kale (*Brassica oleracea* L. *ssp. acephala* L. var*. sabellica*) induces apoptosis in human colorectal cancer cells *in vitro*. *Molecules* **28**, 6938 (2023).
5. Bowen-Forbes, C. *et al.* Broccoli, kale, and radish sprouts: key phytochemical constituents and DPPH free radical scavenging activity. *Molecules* **28**, 4266 (2023).
6. Cao, D. *et al.* Spermidine enhances chilling tolerance of kale seeds by modulating ROS and phytohormone metabolism. *PLOS ONE* **18**, e0289563 (2023).
7. Bauer, N. *et al.* Mechanisms of kale (*Brassica oleracea var. acephala*) tolerance to individual and combined stresses of drought and elevated temperature. *Int. J. Mol. Sci.* **23**, 11494 (2022).
8. Fussy, A. & Papenbrock, J. An overview of soil and soilless cultivation techniques—chances, challenges and the neglected question of sustainability. *Plants* **11**, 1153 (2022).
9. https://www.alliedmarketresearch.com, A. M. R. Kale Microgreen Market Size, Share, Price, Trends |Research Report 2030. *Allied Market Research* https://www.alliedmarketresearch.com/kale-microgreen-market-A16137.
10. Avgoustaki, D. D. & Xydis, G. Chapter One - How energy innovation in indoor vertical farming can improve food security, sustainability, and food safety? in *Advances in Food Security and Sustainability* (ed. Cohen, M. J.) vol. 5 1–51 (Elsevier, 2020).
11. Hati, A. J. & Singh, R. R. Smart indoor farms: Leveraging technological advancements to power a sustainable agricultural revolution. *AgriEngineering* **3**, 728–767 (2021).
12. Nájera, C., Gallegos-Cedillo, V. M., Ros, M. & Pascual, J. A. LED lighting in vertical farming systems enhances bioactive compounds and productivity of vegetables crops. *Biol. Life Sci. Forum* **16**, 24 (2022).
13. Ma, Y., Xu, A. & Cheng, Z.-M. (Max). Effects of light emitting diode lights on plant growth, development and traits a meta-analysis. *Hortic. Plant J.* **7**, 552–564 (2021).
14. McCree, K. J. The action spectrum, absorptance and quantum yield of photosynthesis in crop plants. *Agric. Meteorol.* **9**, 191–216 (1971).
15. Krahmer, J., Ganpudi, A., Abbas, A., Romanowski, A. & Halliday, K. J. Phytochrome, carbon sensing, metabolism, and plant growth plasticity. *Plant Physiol.* **176**, 1039–1048 (2018).
16. Chen, J. *et al.* Effect of photoperiod on chinese kale (*Brassica alboglabra*) sprouts under white or combined red and blue light. *Front. Plant Sci.* **11**, (2021).
17. Kong, Y., Schiestel, K. & Zheng, Y. Pure blue light effects on growth and morphology are slightly changed by adding low-level UVA or far-red light: A comparison with red light in four microgreen species. *Environ. Exp. Bot.* **157**, 58–68 (2019).
18. Deng, M. *et al.* Influence of pre-harvest red light irradiation on main phytochemicals and antioxidant activity of Chinese kale sprouts. *Food Chem.* **222**, 1–5 (2017).
19. Zhen, S. & van Iersel, M. W. Far-red light is needed for efficient photochemistry and photosynthesis. *J. Plant Physiol.* **209**, 115–122 (2017).

20. Furuya, M. & Schäfer, E. Photoperception and signalling of induction reactions by different phytochromes. *Trends Plant Sci.* **1**, 301–307 (1996).
21. Scandola, S., Mehta, D., Castillo, B., Boyce, N. & Uhrig, R. G. Systems-level proteomics and metabolomics reveals the diel molecular landscape of diverse kale cultivars. *Front. Plant Sci.* **14**, (2023).
22. Kuhlgert, S. *et al.* MultispeQ Beta: a tool for large-scale plant phenotyping connected to the open PhotosynQ network. *R. Soc. Open Sci.* **3**, 160592 (2016).
23. Gehan, M. A. *et al.* PlantCV v2: Image analysis software for high-throughput plant phenotyping. *PeerJ* **5**, e4088 (2017).
24. Mehta, D., Scandola, S. & Uhrig, R. G. BoxCar and library-free data-independent acquisition substantially improve the depth, range, and completeness of label-free quantitative proteomics. *Anal. Chem.* **94**, 793–802 (2022).
25. He, J. & Giusti, M. M. Anthocyanins: Natural colorants with health-promoting properties. *Annu. Rev. Food Sci. Technol.* **1**, 163–187 (2010).
26. Zhang, Y., Butelli, E. & Martin, C. Engineering anthocyanin biosynthesis in plants. *Curr. Opin. Plant Biol.* **19**, 81–90 (2014).
27. Genty, B., Briantais, J.-M. & Baker, N. R. The relationship between the quantum yield of photosynthetic electron transport and quenching of chlorophyll fluorescence. *Biochim. Biophys. Acta BBA - Gen. Subj.* **990**, 87–92 (1989).
28. Baker, N. R., Harbinson, J. & Kramer, D. M. Determining the limitations and regulation of photosynthetic energy transduction in leaves. *Plant Cell Environ.* **30**, 1107–1125 (2007).
29. Asher, A. H. & Theg, S. M. Electrochromic shift supports the membrane destabilization model of Tat-mediated transport and shows ion leakage during Sec transport. *Proc. Natl. Acad. Sci.* **118**, e2018122118 (2021).
30. Mallhi, Z. I. *et al.* Citric acid enhances plant growth, photosynthesis, and phytoextraction of lead by alleviating the oxidative stress in castor beans. *Plants* **8**, 525 (2019).
31. Eckardt, N. A. Myo-Inositol biosynthesis genes in Arabidopsis: Differential patterns of gene expression and role in cell death. *Plant Cell* **22**, 537 (2010).
32. Castonguay, A. C., Olson, L. J. & Dahms, N. M. Mannose 6-phosphate receptor homology (MRH) domain-containing lectins in the secretory pathway. *Biochim. Biophys. Acta BBA - Gen. Subj.* **1810**, 815–826 (2011).
33. Verbančič, J., Lunn, J. E., Stitt, M. & Persson, S. Carbon supply and the regulation of cell wall synthesis. *Mol. Plant* **11**, 75–94 (2018).
34. Díaz, M., De Haro, V., Muñoz, R. & Quiles, M. J. Chlororespiration is involved in the adaptation of Brassica plants to heat and high light intensity. *Plant Cell Environ.* **30**, 1578–1585 (2007).
35. Cosgrove, D. J. Growth of the plant cell wall. *Nat. Rev. Mol. Cell Biol.* **6**, 850–861 (2005).
36. Wilson, L. F. L. *et al.* The biosynthesis, degradation, and function of cell wall β-xylosylated xyloglucan mirrors that of arabinoxyloglucan. *New Phytol.* **240**, 2353–2371 (2023).
37. Tong, L. *et al.* Powerful cell wall biomass degradation enzymatic system from saprotrophic Aspergillus fumigatus. *Cell Surf. Amst. Neth.* **11**, 100126 (2024).
38. Kamal, K. Y. *et al.* Evaluation of growth and nutritional value of Brassica microgreens grown under red, blue and green LEDs combinations. *Physiol. Plant.* **169**, 625–638 (2020).
39. He, R. *et al.* The combination of selenium and LED light quality affects growth and nutritional properties of broccoli sprouts. *Molecules* **25**, 4788 (2020).
40. Pierik, R. & de Wit, M. Shade avoidance: phytochrome signalling and other aboveground neighbour detection cues. *J. Exp. Bot.* **65**, 2815–2824 (2014).

41. Paik, I. & Huq, E. Plant photoreceptors: Multi-functional sensory proteins and their signaling networks. *Semin. Cell Dev. Biol.* **92**, 114–121 (2019).
42. Liu, W. *et al.* Phosphorylation of Arabidopsis UVR8 photoreceptor modulates protein interactions and responses to UV-B radiation. *Nat. Commun.* **15**, 1221 (2024).
43. Liu, X. *et al.* FERONIA coordinates plant growth and salt tolerance via the phosphorylation of phyB. *Nat. Plants* **9**, 645–660 (2023).
44. Viczián, A. *et al.* Differential phosphorylation of the N-terminal extension regulates phytochrome B signaling. *New Phytol.* **225**, 1635–1650 (2020).
45. Gao, L. *et al.* Blue light-induced phosphorylation of Arabidopsis cryptochrome 1 is essential for its photosensitivity. *J. Integr. Plant Biol.* **64**, 1724–1738 (2022).
46. Schumacher, P. *et al.* A phosphorylation switch turns a positive regulator of phototropism into an inhibitor of the process. *Nat. Commun.* **9**, 2403 (2018).
47. Inoue, S. *et al.* Blue light-induced autophosphorylation of phototropin is a primary step for signaling. *Proc. Natl. Acad. Sci.* **105**, 5626–5631 (2008).
48. Balázs, L. *et al.* Quantifying the effect of light intensity uniformity on the crop yield by pea microgreens growth experiments. *Horticulturae* **9**, 1187 (2023).
49. Jones-Baumgardt, C., Llewellyn, D., Ying, Q. & Zheng, Y. Intensity of sole-source light-emitting diodes affects growth, yield, and quality of Brassicaceae microgreens. (2019) doi:10.21273/HORTSCI13788-18.
50. Dou, H. *et al.* Supplementary far-red light for photosynthetic active radiation differentially influences the photochemical efficiency and biomass accumulation in greenhouse-grown lettuce. *Plants* **13**, 2169 (2024).
51. Frąszczak, B. *et al.* Morphological and photosynthetic parameters of green and red kale microgreens cultivated under different light spectra. *Plants* **12**, 3800 (2023).
52. Bancos, S. *et al.* Diurnal regulation of the brassinosteroid-biosynthetic CPD gene in Arabidopsis. *Plant Physiol.* **141**, 299–309 (2006).
53. Pan, Y. *et al.* Cytochrome P450 monooxygenases as reporters for circadian-regulated pathways. *Plant Physiol.* **150**, 858–878 (2009).
54. Martínez, C. *et al.* PIF4-induced BR synthesis is critical to diurnal and thermomorphogenic growth. *EMBO J.* **37**, e99552 (2018).
55. Asahina, M. *et al.* Blue light-promoted rice leaf bending and unrolling are due to up-regulated brassinosteroid biosynthesis genes accompanied by accumulation of castasterone. *Phytochemistry* **104**, 21–29 (2014).
56. Lv, M. & Li, J. Molecular mechanisms of brassinosteroid-mediated responses to changing environments in Arabidopsis. *Int. J. Mol. Sci.* **21**, 2737 (2020).
57. Keuskamp, D. H. *et al.* Blue-light-mediated shade avoidance requires combined auxin and brassinosteroid action in Arabidopsis seedlings. *Plant J.* **67**, 208–217 (2011).
58. Klahre, U. *et al.* The Arabidopsis DIMINUTO/DWARF1 gene encodes a protein involved in steroid synthesis. *Plant Cell* **10**, 1677–1690 (1998).
59. Yun, F., Liu, H., Deng, Y., Hou, X. & Liao, W. The role of light-regulated auxin signaling in root development. *Int. J. Mol. Sci.* **24**, 5253 (2023).
60. Ma, L. & Li, G. Auxin-dependent cell elongation during the shade avoidance response. *Front. Plant Sci.* **10**, (2019).
61. Sasidharan, R. *et al.* Light quality-mediated petiole elongation in Arabidopsis during shade avoidance involves cell wall modification by xyloglucan endotransglucosylase/hydrolases. *Plant Physiol.* **154**, 978–990 (2010).

62. Sasidharan, R., Chinnappa, C. C., Voesenek, L. A. C. J. & Pierik, R. The regulation of cell wall extensibility during shade avoidance: a study using two contrasting ecotypes of *Stellaria longipes*. *Plant Physiol.* **148**, 1557–1569 (2008).
63. Teramoto, H., Nakamori, A., Minagawa, J. & Ono, T. Light-intensity-dependent expression of Lhc gene family encoding light-harvesting chlorophyll-a/b proteins of photosystem II in *Chlamydomonas reinhardtii*. *Plant Physiol.* **130**, 325–333 (2002).
64. Anderson, J. M., Chow, W. S. & Goodchild, D. J. Thylakoid membrane organisation in sun/shade acclimation. *Funct. Plant Biol.* **15**, 11–26 (1988).
65. Anderson, J. M., Chow, W. S. & Park, Y.-I. The grand design of photosynthesis: Acclimation of the photosynthetic apparatus to environmental cues. *Photosynth. Res.* **46**, 129–139 (1995).
66. Jin, D. *et al.* Effect of red and blue light on cucumber seedlings grown in a plant factory. *Horticulturae* **9**, 124 (2023).
67. Podsędek, A. Natural antioxidants and antioxidant capacity of Brassica vegetables: A review. *LWT - Food Sci. Technol.* **40**, 1–11 (2007).
68. Sun, B., Yan, H., Liu, N., Wei, J. & Wang, Q. Effect of 1-MCP treatment on postharvest quality characters, antioxidants and glucosinolates of Chinese kale. *Food Chem.* **131**, 519–526 (2012).
69. Liu, K. *et al.* Light intensity and photoperiod affect growth and nutritional quality of Brassica microgreens. *Molecules* **27**, 883 (2022).
70. Tena, N., Martín, J. & Asuero, A. G. State of the art of anthocyanins: antioxidant activity, sources, bioavailability, and therapeutic effect in human health. *Antioxidants* **9**, 451 (2020).
71. Pojer, E., Mattivi, F., Johnson, D. & Stockley, C. S. The case for anthocyanin consumption to promote human health: A review. *Compr. Rev. Food Sci. Food Saf.* **12**, 483–508 (2013).
72. Liu, C., Yao, X., Li, G., Huang, L. & Xie, Z. Transcriptomic profiling of purple broccoli reveals light-induced anthocyanin biosynthetic signaling and structural genes. *PeerJ* **8**, e8870 (2020).
73. Kim, C. Y. *et al.* Emergence of a proton exchange-based isomerization and lactonization mechanism in the plant coumarin synthase COSY. *Nat. Commun.* **14**, 597 (2023).
74. Vanholme, R. *et al.* COSY catalyses trans–cis isomerization and lactonization in the biosynthesis of coumarins. *Nat. Plants* **5**, 1066–1075 (2019).
75. Rani, S. H., Krishna, T. H. A., Saha, S., Negi, A. S. & Rajasekharan, R. Defective in Cuticular Ridges (*DCR*) of *Arabidopsis thaliana*, a gene associated with surface cutin formation, encodes a soluble diacylglycerol acyltransferase*. *J. Biol. Chem.* **285**, 38337–38347 (2010).
76. Agerbirk, N. & Olsen, C. E. Glucosinolate structures in evolution. *Phytochemistry* **77**, 16–45 (2012).
77. Biegańska-Marecik, R., Radziejewska-Kubzdela, E. & Marecik, R. Characterization of phenolics, glucosinolates and antioxidant activity of beverages based on apple juice with addition of frozen and freeze-dried curly kale leaves (*Brassica oleracea* L. var. *acephala* L.). *Food Chem.* **230**, 271–280 (2017).
78. Ltd, wflpublisher. Comparative study on functional components, antioxidant activity and color parameters of selected colored leafy vegetables as affected by photoperiods. *wflpublisher.com* https://www.wflpublisher.com/Abstract/2605.
79. Park, C. H. *et al.* Effects of light-emitting diodes on the accumulation of glucosinolates and phenolic compounds in sprouting canola (*Brassica napus L.*). *Foods* **8**, 76 (2019).

80. Zhou, B. *et al.* Effects of light intensity on the biosynthesis of glucosinolate in Chinese cabbage plantlets. *Sci. Hortic.* **316**, 112036 (2023).
81. Eggersdorfer, M. & Wyss, A. Carotenoids in human nutrition and health. *Arch. Biochem. Biophys.* **652**, 18–26 (2018).
82. Flores, M., Hernández-Adasme, C., Guevara, M. J. & Escalona, V. H. Effect of different light intensities on agronomic characteristics and antioxidant compounds of Brassicaceae microgreens in a vertical farm system. *Front. Sustain. Food Syst.* **8**, (2024).
83. Simkin, A. J., Zhu, C., Kuntz, M. & Sandmann, G. Light-dark regulation of carotenoid biosynthesis in pepper (*Capsicum annuum*) leaves. *J. Plant Physiol.* **160**, 439–443 (2003).
84. Pizarro, L. & Stange, C. Light-dependent regulation of carotenoid biosynthesis in plants. *Cienc. E Investig. Agrar.* **36**, 143–162 (2009).
85. Lisiewska, Z., Kmiecik, W. & Korus, A. The amino acid composition of kale (*Brassica oleracea* L. var. *acephala*), fresh and after culinary and technological processing. *Food Chem.* **108**, 642–648 (2008).
86. Okumoto, S., Funck, D., Trovato, M. & Forlani, G. Editorial: Amino acids of the glutamate family: functions beyond primary metabolism. *Front. Plant Sci.* **7**, (2016).
87. Kavi Kishor, P. B. & Sreenivasulu, N. Is proline accumulation per se correlated with stress tolerance or is proline homeostasis a more critical issue? *Plant Cell Environ.* **37**, 300–311 (2014).
88. Galili, G. & Amir, R. Fortifying plants with the essential amino acids lysine and methionine to improve nutritional quality. *Plant Biotechnol. J.* **11**, 211–222 (2013).
89. Yang, Q., Zhao, D. & Liu, Q. Connections between amino acid metabolisms in plants: lysine as an example. *Front. Plant Sci.* **11**, (2020).
90. Hall, C. J. *et al.* Differential lysine-mediated allosteric regulation of plant dihydrodipicolinate synthase isoforms. *FEBS J.* **288**, 4973–4986 (2021).
91. Van Bochaute, P., Novoa, A., Ballet, S., Rognes, S. E. & Angenon, G. Regulatory mechanisms after short- and long-term perturbed lysine biosynthesis in the aspartate pathway: the need for isogenes in Arabidopsis thaliana. *Physiol. Plant.* **149**, 449–460 (2013).
92. Stein, O. & Granot, D. An overview of sucrose synthases in plants. *Front. Plant Sci.* **10**, (2019).
93. Hwang, G. *et al.* Trehalose-6-phosphate signaling regulates thermoresponsive hypocotyl growth in Arabidopsis thaliana. *EMBO Rep.* **20**, e47828 (2019).
94. Avidan, O. *et al.* Direct and indirect responses of the Arabidopsis transcriptome to an induced increase in trehalose 6-phosphate. *Plant Physiol.* **196**, 409–431 (2024).
95. Sharma, N., Chaudhary, C. & Khurana, P. Role of myo-inositol during skotomorphogenesis in Arabidopsis. *Sci. Rep.* **10**, 17329 (2020).
96. Godoy Herz, M. A. *et al.* Light regulates plant alternative splicing through the control of transcriptional elongation. *Mol. Cell* **73**, 1066-1074.e3 (2019).

FIGURES

Figure 1. Effect of light intensities and spectra on kale growth and development.
A. Pictures of K3 and K9 plants at 35 dpi grown under different light intensities (75, 125, and 175 PPFD).

B. K3 and K9 weight at 35 dpi (n=6), leaf area at 22 dpi (n=15) and K9 anthocyanin content at 35 dpi (n=4), at different light intensities (75, 125, and 175 PPFD).
C. Pictures of K3 and K9 plants at different light spectra (low, balanced, high R/B and R/FR) grown for 35 dpi.
D. K3 and K9 weight at 35 dpi (n=6), leaf area at 22 dpi (n=28) and K9 anthocyanin content at 35 dpi (n=4), at different light spectra (low, balanced, high R/B and R/FR).
Letters shows significant differences using a one-way ANOVA and Tukey's post-hoc test (adjusted p-value <0.05).

Figure 2. Effect of Light Intensity and spectra on Photosynthetic Parameters Measured with MultispeQ.
A. Light intensity effect on relative chlorophyll content (SPAD) and photosynthetic parameters (Phi2, PhiNO, PhiNPQ) were measured with MultispeQ at 35 dpi (n=10).
B. Light spectra effect on relative chlorophyll content (SPAD) and photosynthetic parameters (Phi2, PhiNO, PhiNPQ) were measured with MultispeQ at 35 dpi (n=10).
Letters show significant differences using a one-way ANOVA and Tukey's post-hoc test (adjusted p-value < 0.05).

Figure 3. Effect of light intensity treatment on the metabolite composition of Kale cultivars.
GC-MS analysis of primary metabolites in kale cultivars K3 and K9 under different light intensity 75, 125 and 175 PPFD and at ZT11 / ZT23 (n=4). Different letters indicate significant differences using a one-way ANOVA and Tukey's post-hoc test (adjusted p-value < 0.05).

Figure 4. Effect of light spectra treatment on the metabolite composition of Kale cultivars.
GC-MS analysis of primary metabolites in kale cultivars K3 and K9 under different light spectra (low, balanced and high R/B) and at ZT11 / ZT23 (n=4). Different letters indicate significant differences using a one-way ANOVA and Tukey's post-hoc test (adjusted p-value < 0.05).

Figure 5. Effect of light spectra treatment on the metabolite composition of Kale cultivars.
GC-MS analysis of primary metabolites in kale cultivars K3 and K9 under different light spectra (low, balanced and high R/FR) and at ZT11 / ZT23 (n=4). Different letters indicate significant differences using a one-way ANOVA and Tukey's post-hoc test (adjusted p-value < 0.05).

Figure 6. Analysis of significantly changing proteins with changing light intensity and spectral composition.
A-C. Number of proteins with a significant change in abundance with increase in light intensity from 75 PPFD (A), from low R/B (B) and from low R/FR (C).
D. Dot plot representation of enriched GO terms for biological process of significantly changing proteins (q-value < 0.05; Log2FC > 0.58 or < -0.58) that are up- or down-regulated with increasing light intensity (top panel), increasing R/B ratio (middle panel), or increasing R/FR ratio (bottom panel) at ZT23 (left) or ZT11 (right). Dot size indicates the gene ratio (number of proteins in the changing in the condition/total quantified proteins in the category in the study). Dot colour represents the Log10 (p-value). Only GO terms with p-value <0.01 and a total count < 500 are included.

Figure 7. Association network analysis of significantly changing proteins with increasing light intensity

An association network analysis was performed using STRING-DB to depict significantly changing proteins in K3 and K9 kale under increasing light intensity at ZT23 and ZT11. Edge thickness indicates strength of connection between the nodes. Minimum edge threshold was set to 0.95. Protein nodes are labelled either by primary gene name or Arabidopsis gene identifier (AGI). Outer circle surrounding each node represents the standardized relative Log2FC of the indicated significantly changing protein with an increase from 75 PPFD to either 125 PPFD or 175 PPFD in K3 or K9 as indicated by the legend. The scale of blue to yellow indicates the relative decrease or increase in abundance, respectively from 75 PPFD to either 125 PPFD or 175 PPFD. Node groupings are indicated by a grey circle representing proteins involved in the same biological process.

Figure 8. Association network analysis of significantly changing proteins with changing light quality

An association network analysis was performed using STRING-DB to depict significantly changing proteins in K3 and K9 kale under increasing R/B spectral ratio (A) or R/FR ratio (B) at ZT23 and ZT11. Edge thickness indicates the strength of connection between the nodes. Minimum edge threshold was set to 0.95. Protein nodes are labelled either by primary gene name or Arabidopsis gene identifier (AGI). Outer circle surrounding each node represents the standardized relative Log2FC of the indicated significantly changing protein with an increase from low R/B (A) or low R/FR (B) to balanced R/B (R = B) or high R/B (R > B) (A) or balanced R/FR (R = FR) or high R/FR (R > FR) (B) in K3 or K9 at ZT23 or ZT11 as indicated by the legend. The scale of blue to yellow indicates the relative decrease or increase in abundance, respectively. Node groupings are indicated by a grey circle representing proteins involved in the same biological process.

SUPPLEMENTAL DATA

Table S1. Gas chromatography metabolite data for Intensity experiments

Table S2. Gas chromatography metabolite data for Spectra experiments

Table S3. Liquid chromatography proteomic data

Table S4. Pathway enrichment analysis using the Plant Metabolic Network (PMN; https://plantcyc.org) for Intensity experiments

Table S5. Pathway enrichment analysis using the Plant Metabolic Network (PMN; https://plantcyc.org) for R/B Spectra experiments

Table S6. Pathway enrichment analysis using the Plant Metabolic Network (PMN; https://plantcyc.org) for R/FR Spectra experiments

Supplemental Figure 1. Light spectra of the different light treatments

A. Light spectra of different light intensity (75, 125 and 175 PPFD).
B. Light spectra of the different light ratios (low R/B, balanced and high R/FR). Light intensity is 125 PPFD for all spectra treatment.

Supplemental Figure 2: Effect of Light Intensity and spectra on Photosynthetic Parameters Measured with MultispeQ.
A. Light intensity effect on photosynthetic parameters (LEF, gH+, ECSt, vH+) were measured with MultispeQ at 35 dpi (n=10).
B. Light spectra effect on photosynthetic parameters (LEF, gH+, ECSt, vH+) were measured with MultispeQ at 35 dpi (n=10).
Letters show significant differences using a one-way ANOVA and Tukey's post-hoc test (adjusted p-value < 0.05).

Supplemental Figure 3: GC-MS analysis of kale cultivars K3 and K9 under different light intensities (75 PPFD, 125 PPFD and 175 PPFD) and at different time of the day (ZT11 and ZT23).
A. Heatmap of relative cultivars metabolite changes at ZT11 and ZT23.
B. Eucledian distance clustered heatmap of relative cultivars metabolite changes.
C. Heatmap of relative diel metabolite changes in K3 and K9.
D.Eucledian distance clustered heatmap of relative diel metabolite changes in K3 and K9.
Heatmaps were generated using the R package *Pheatmaps*. Scale represents Log2 fold-change (FC); n=4.

Supplemental Figure 4: GC-MS analysis of kale cultivars K3 and K9 under different light spectra (low, balanced, and high R/B ratios) and at different time of the day (ZT11 and ZT23).
A. Heatmap of relative cultivars metabolite changes at ZT11 and ZT23.
B. Eucledian distance clustered heatmap of relative cultivars metabolite changes.
C. Heatmap of relative diel metabolite changes in K3 and K9.
D. Eucledian distance clustered heatmap of relative diel metabolite changes in K3 and K9.
Heatmaps were generated using the R package *Pheatmaps*. Scale represents Log2 fold-change (FC); n=4.

Supplemental Figure 5: GC-MS analysis of kale cultivars K3 and K9 under different light spectra (low, balanced, and high R/FR ratios) and at different time of the day (ZT11 and ZT23).
A. Heatmap of relative cultivars metabolite changes at ZT11 and ZT23.
B. Eucledian distance clustered heatmap of relative cultivars metabolite changes.
C. Heatmap of relative diel metabolite changes in K3 and K9.
D. Eucledian distance clustered heatmap of relative diel metabolite changes in K3 and K9.
Heatmaps were generated using the R package *Pheatmaps*. Scale represents Log2 fold-change (FC); n=4.

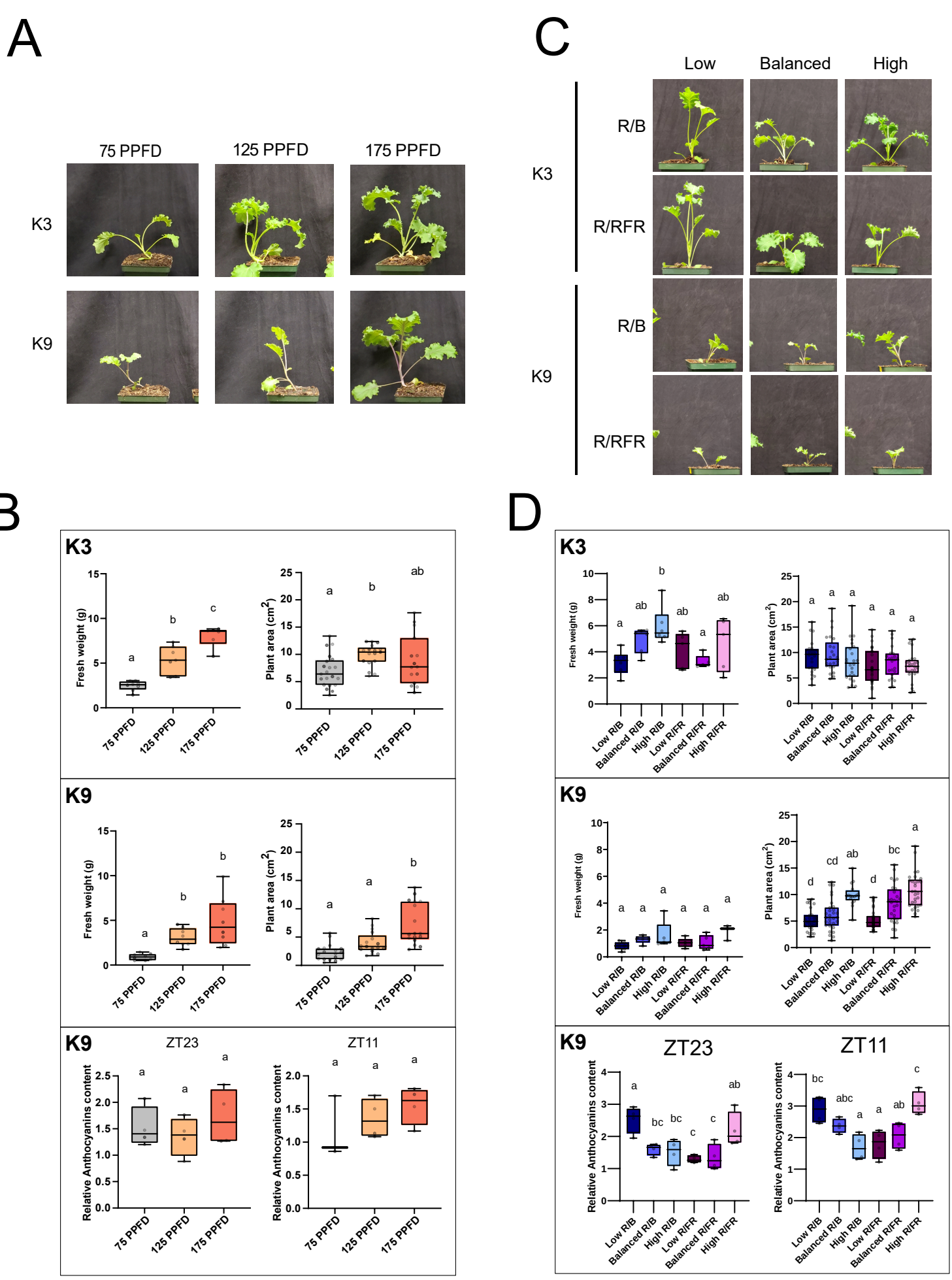

Figure 1. Effect of light intensities and spectra on kale growth and development.
A. Pictures of K3 and K9 plants at 35 dpi grown under different light intensities (75, 125, and 175 PPFD).
B. K3 and K9 weight at 35 dpi (n=6), leaf area at 22 dpi (n=15) and K9 anthocyanin content at 35 dpi (n=4), at different light intensities (75, 125, and 175 PPFD).
C. Pictures of K3 and K9 plants at different light spectra (low, balanced, high R/B and R/FR) grown for 35 dpi.
D. K3 and K9 weight at 35 dpi (n=6), leaf area at 22 dpi (n=28) and K9 anthocyanin content at 35 dpi (n=4), at different light spectra (low, balanced, high R/B and R/FR).
Letters shows significant differences using a one-way ANOVA and Tukey's post-hoc test (adjusted p-value <0.05).

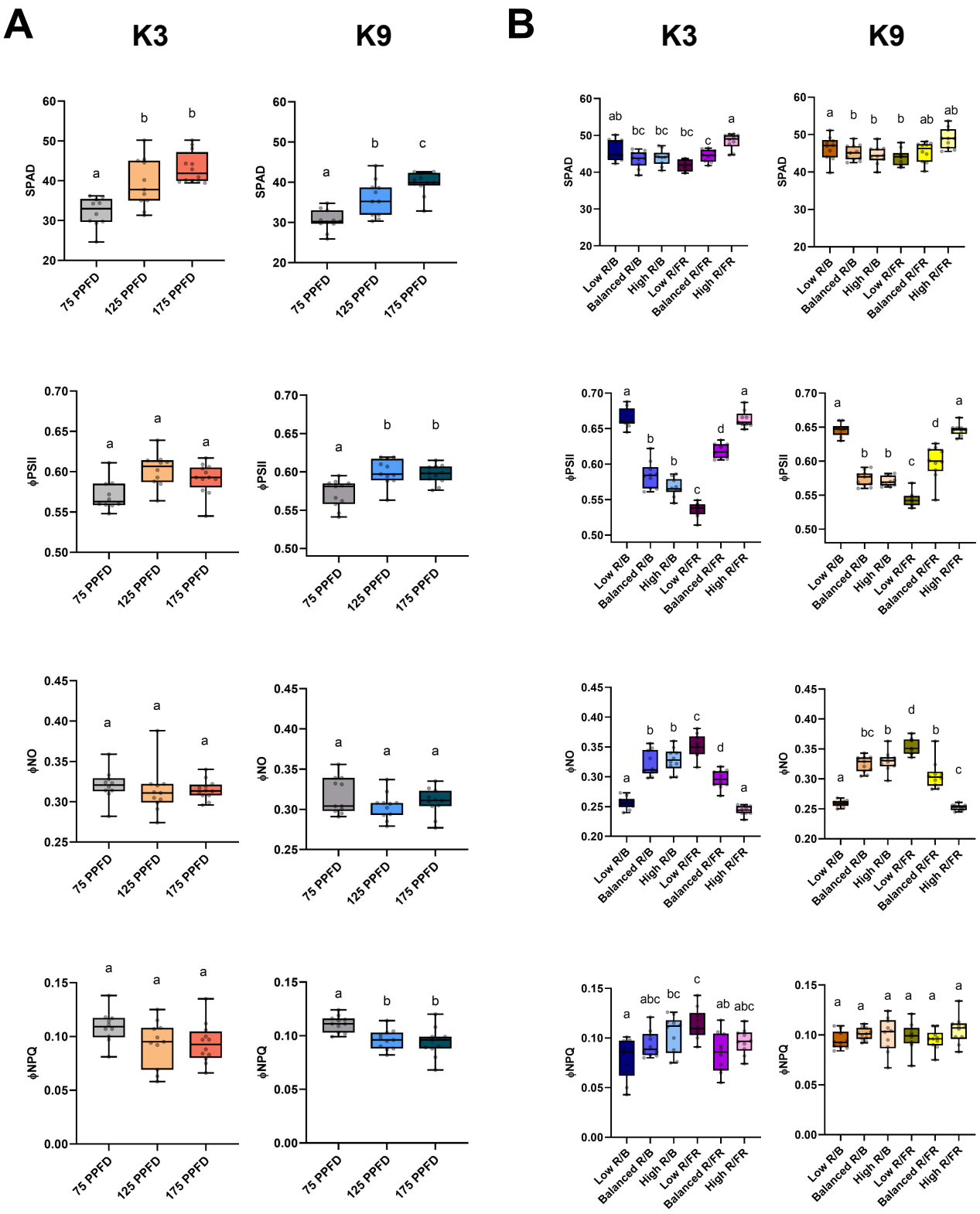

Figure 2. Effect of Light Intensity and spectra on Photosynthetic Parameters Measured with MultispeQ.

A.Light intensity effect on relative chlorophyll content (SPAD) and photosynthetic parameters (Phi2, PhiNO, PhiNPQ) were measured with MultispeQ at 35 dpi (n=10).
B.Light spectra effect on relative chlorophyll content (SPAD) and photosynthetic parameters (Phi2, PhiNO, PhiNPQ) were measured with MultispeQ at 35 dpi (n=10).
Letters show significant differences using a one-way ANOVA and Tukey's post-hoc test (adjusted p-value < 0.05).

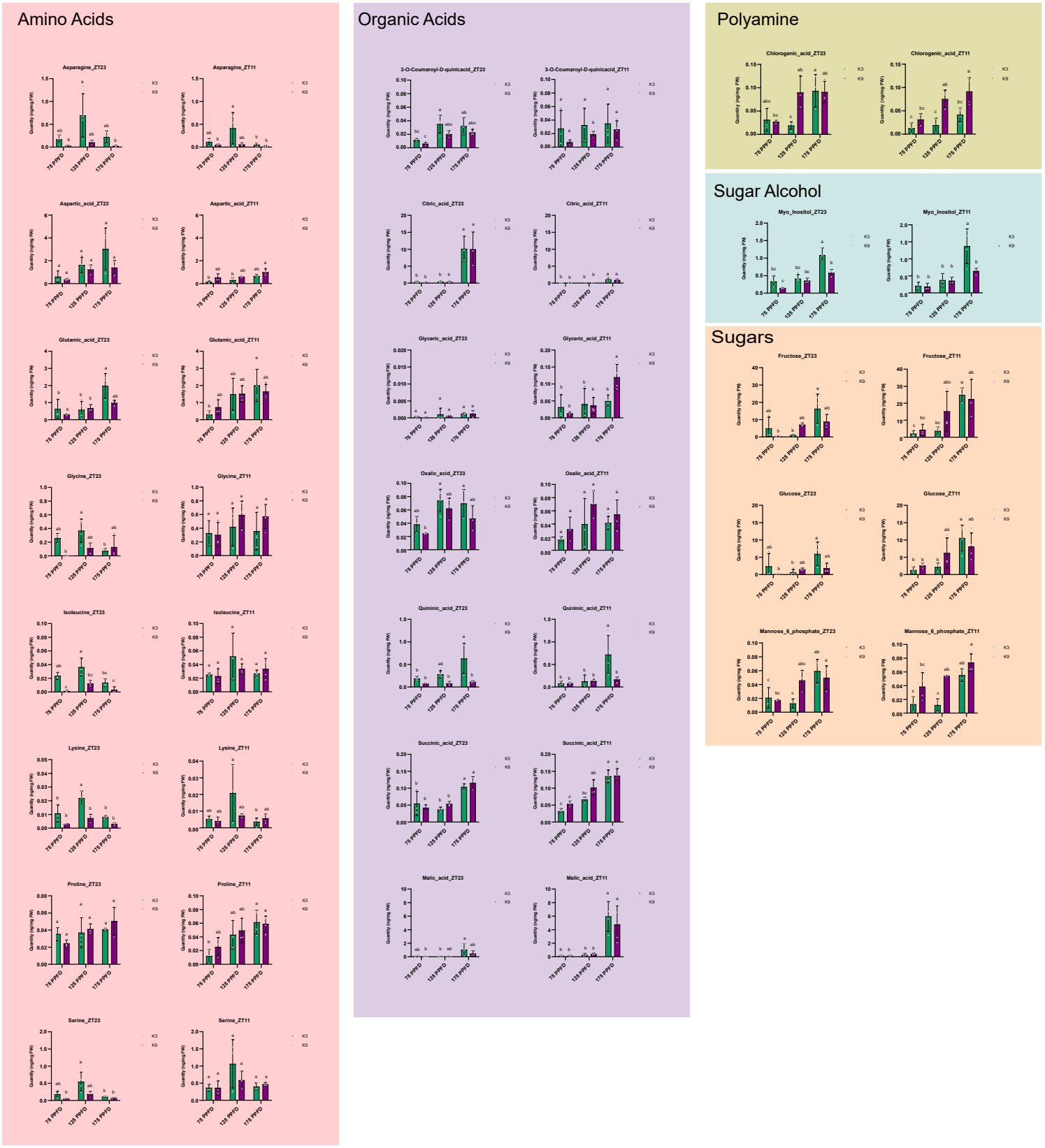

Figure 3. Effect of light intensity treatment on the metabolite composition of Kale cultivars.

GC-MS analysis of primary metabolites in kale cultivars K3 and K9 under different light intensity 75, 125 and 175 PPFD and at ZT11 / ZT23 (n=4). Different letters indicate significant differences using a one-way ANOVA and Tukey's post-hoc test (adjusted p-value < 0.05).

Figure 4. Effect of light spectra treatment on the metabolite composition of Kale cultivars. GC-MS analysis of primary metabolites in kale cultivars K3 and K9 under different light spectra (low, balanced and high R/B) and at ZT11 / ZT23 (n=4). Different letters indicate significant differences using a one-way ANOVA and Tukey's post-hoc test (adjusted p-value < 0.05).

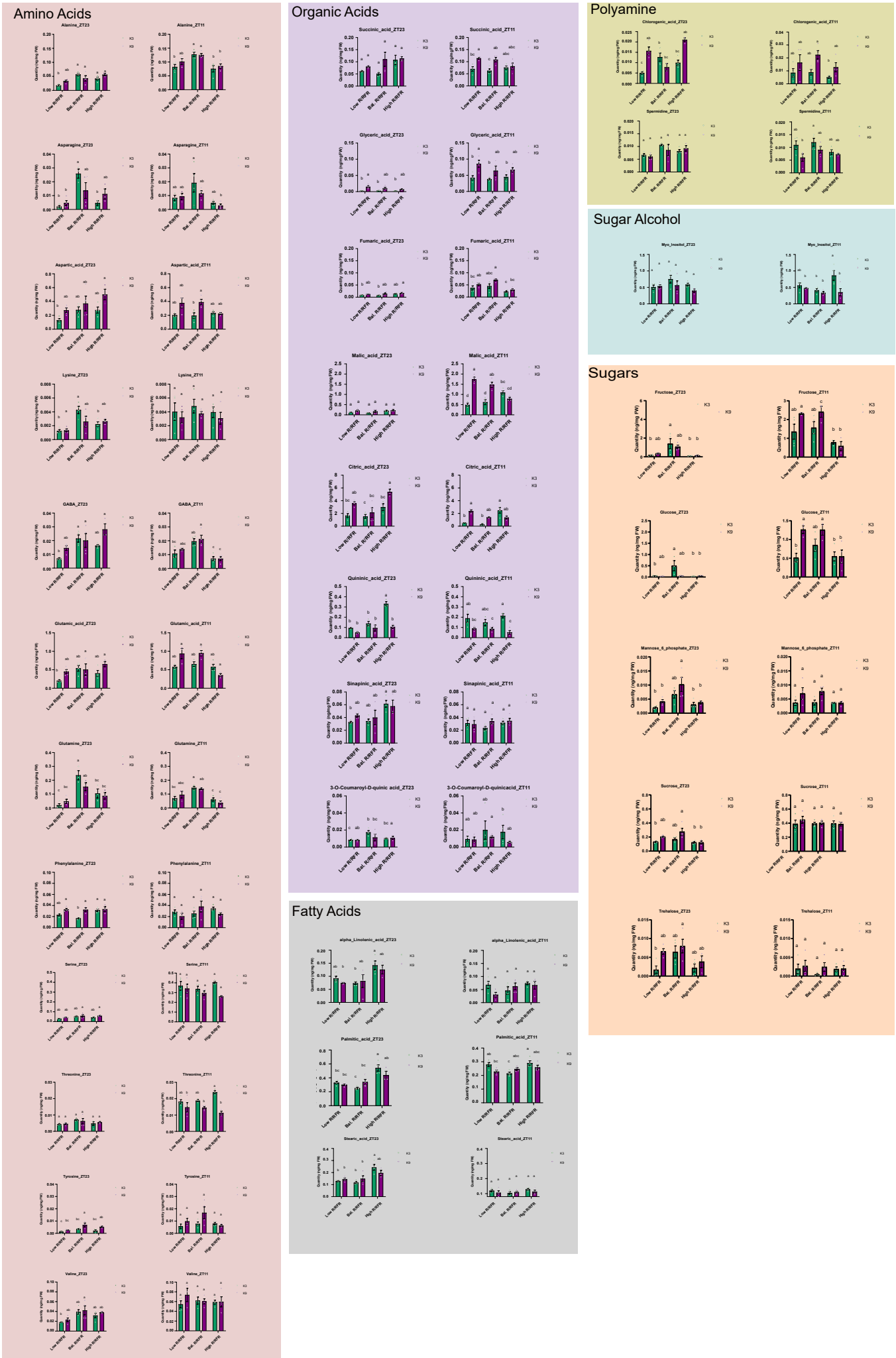

Figure 5. Effect of light spectra treatment on the metabolite composition of Kale cultivars. GC-MS analysis of primary metabolites in kale cultivars K3 and K9 under different light spectra (low, balanced and high R/FR) and at ZT11 / ZT23 (n=4). Different letters indicate significant differences using a one-way ANOVA and Tukey's post-hoc test (adjusted p-value < 0.05).

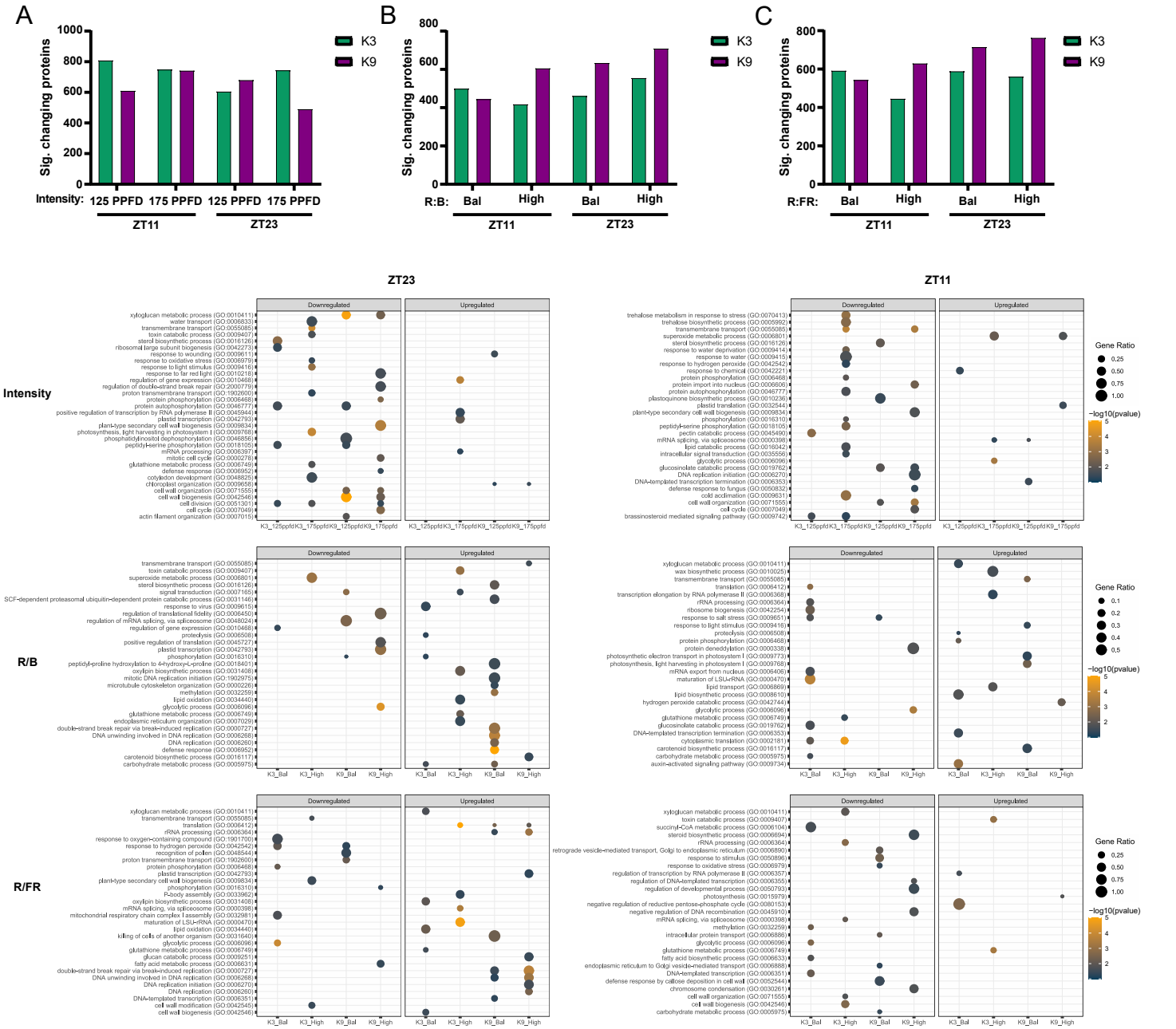

Figure 6. Analysis of significantly changing proteins with changing light intensity and spectral composition.

A-C. Number of proteins with a significant change in abundance with increase in light intensity from 75 PPFD (A), from low R/B (B) and from low R/FR (C).

D. Dot plot representation of enriched GO terms for biological process of significantly changing proteins (q-value < 0.05; Log2FC > 0.58 or < -0.58) that are up- or down-regulated with increasing light intensity (top panel), increasing R/B ratio (middle panel), or increasing R/FR ratio (bottom panel) at ZT23 (left) or ZT11 (right). Dot size indicates the gene ratio (number of proteins in the changing in the condition/total quantified proteins in the category in the study). Dot colour represents the Log10 (p-value). Only GO terms with p-value <0.01 and a total count < 500 are included.

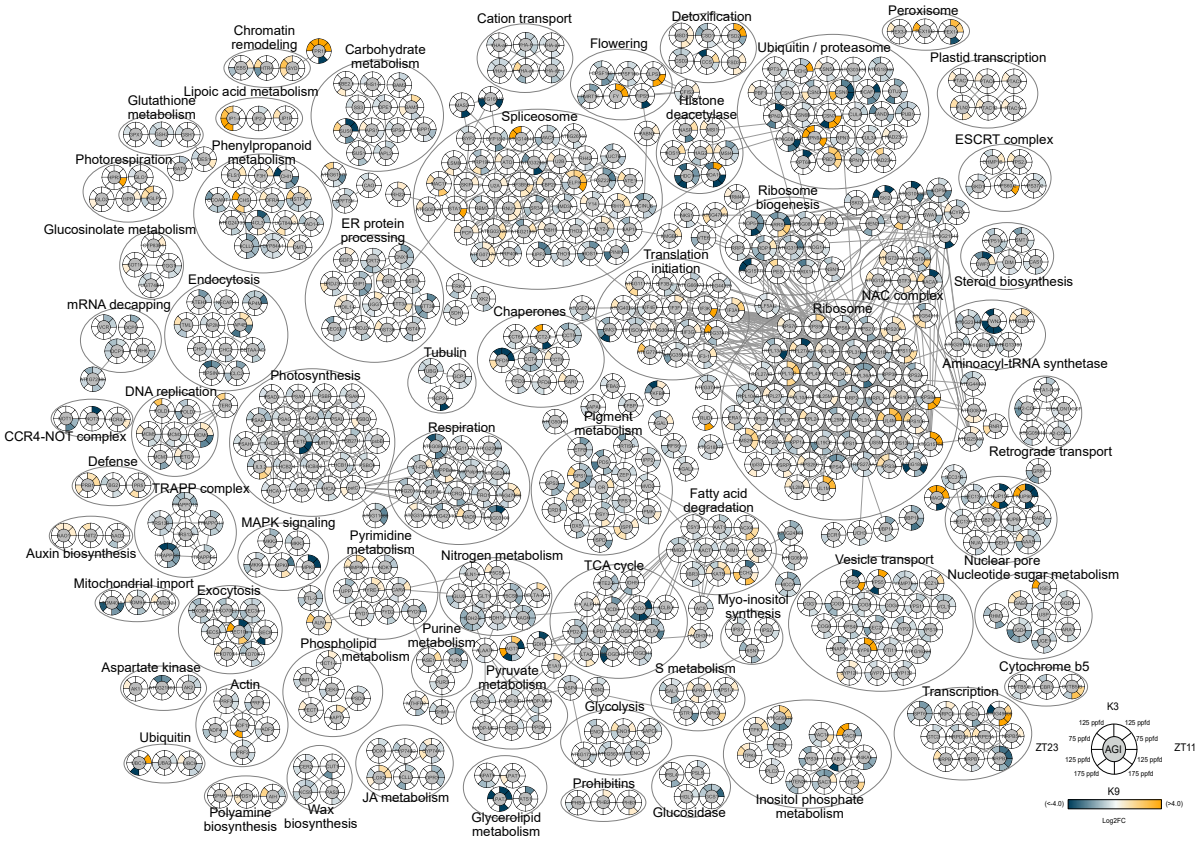

Figure 7. Association network analysis of significantly changing proteins with increasing light intensity.
An association network analysis was performed using STRING-DB to depict significantly changing proteins in K3 and K9 kale under increasing light intensity at ZT23 and ZT11. Edge thickness indicates strength of connection between the nodes. Minimum edge threshold was set to 0.95. Protein nodes are labelled either by primary gene name or Arabidopsis gene identifier (AGI). Outer circle surrounding each node represents the standardized relative Log2FC of the indicated significantly changing protein with an increase from 75 PPFD to either 125 PPFD or 175 PPFD in K3 or K9 as indicated by the legend. The scale of blue to yellow indicates the relative decrease or increase in abundance, respectively from 75 PPFD to either 125 PPFD or 175 PPFD. Node groupings are indicated by a grey circle representing proteins involved in the same biological process.

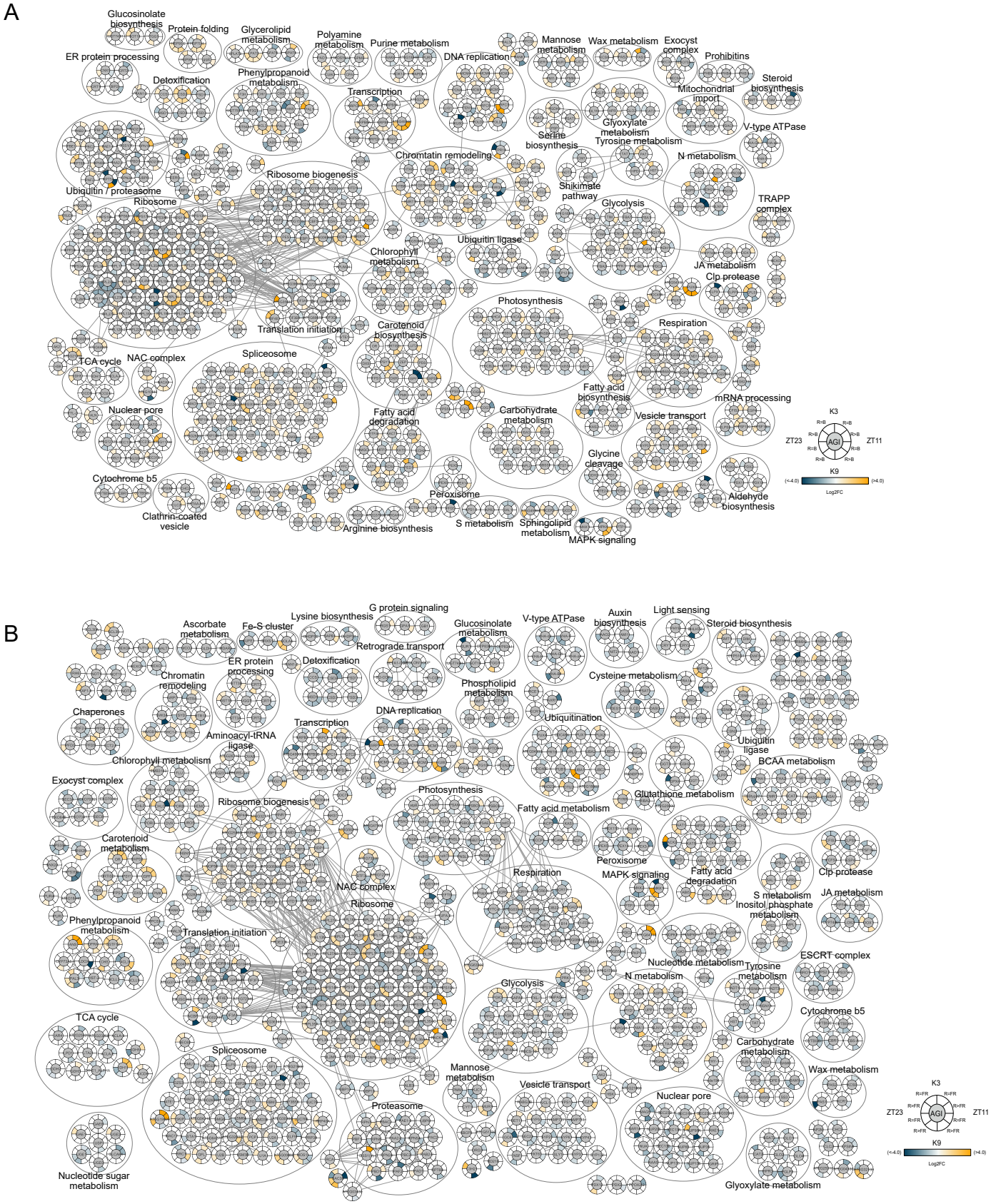

Figure 8. Association network analysis of significantly changing proteins with changing light quality. An association network analysis was performed using STRING-DB to depict significantly changing proteins in K3 and K9 kale under increasing R/B spectral ratio (A) or R/FR ratio (B) at ZT23 and ZT11. Edge thickness indicates the strength of connection between the nodes. Minimum edge threshold was set to 0.95. Protein nodes are labelled either by primary gene name or Arabidopsis gene identifier (AGI). Outer circle surrounding each node represents the standardized relative Log2FC of the indicated significantly changing protein with an increase from low R/B (A) or low R/FR (B) to balanced R/B (R = B) or high R/B (R > B) (A) or balanced R/FR (R = FR) or high R/FR (R > FR) (B) in K3 or K9 at ZT23 or ZT11 as indicated by the legend. The scale of blue to yellow indicates the relative decrease or increase in abundance, respectively. Node groupings are indicated by a grey circle representing proteins involved in the same biological process.

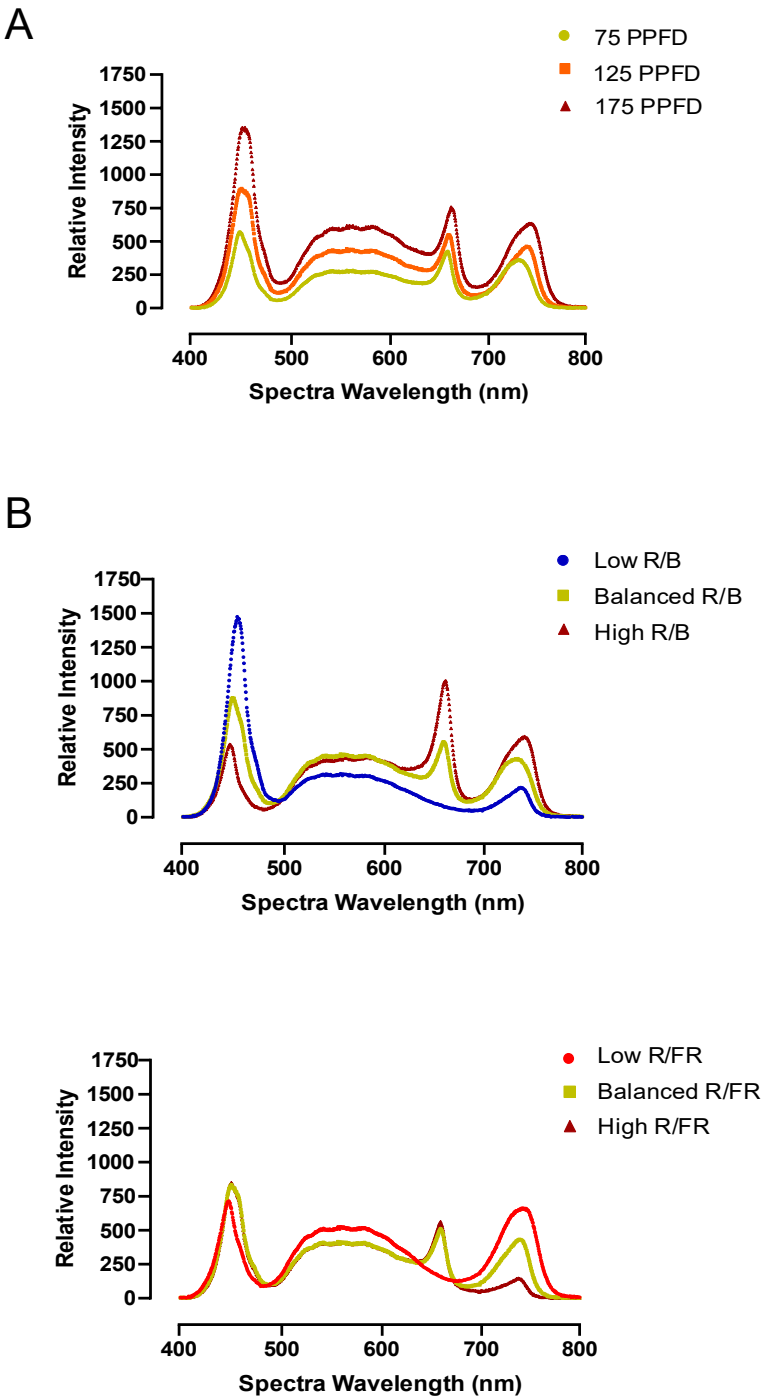

Supplemental Figure 1. Light spectra of the different light treatments.

A. Light spectra of different light intensity (75, 125 and 175 PPFD).
B. Light spectra of the different light ratios (low R/B, balanced and high R/FR). Light intensity is 125 PPFD for all spectra treatment.

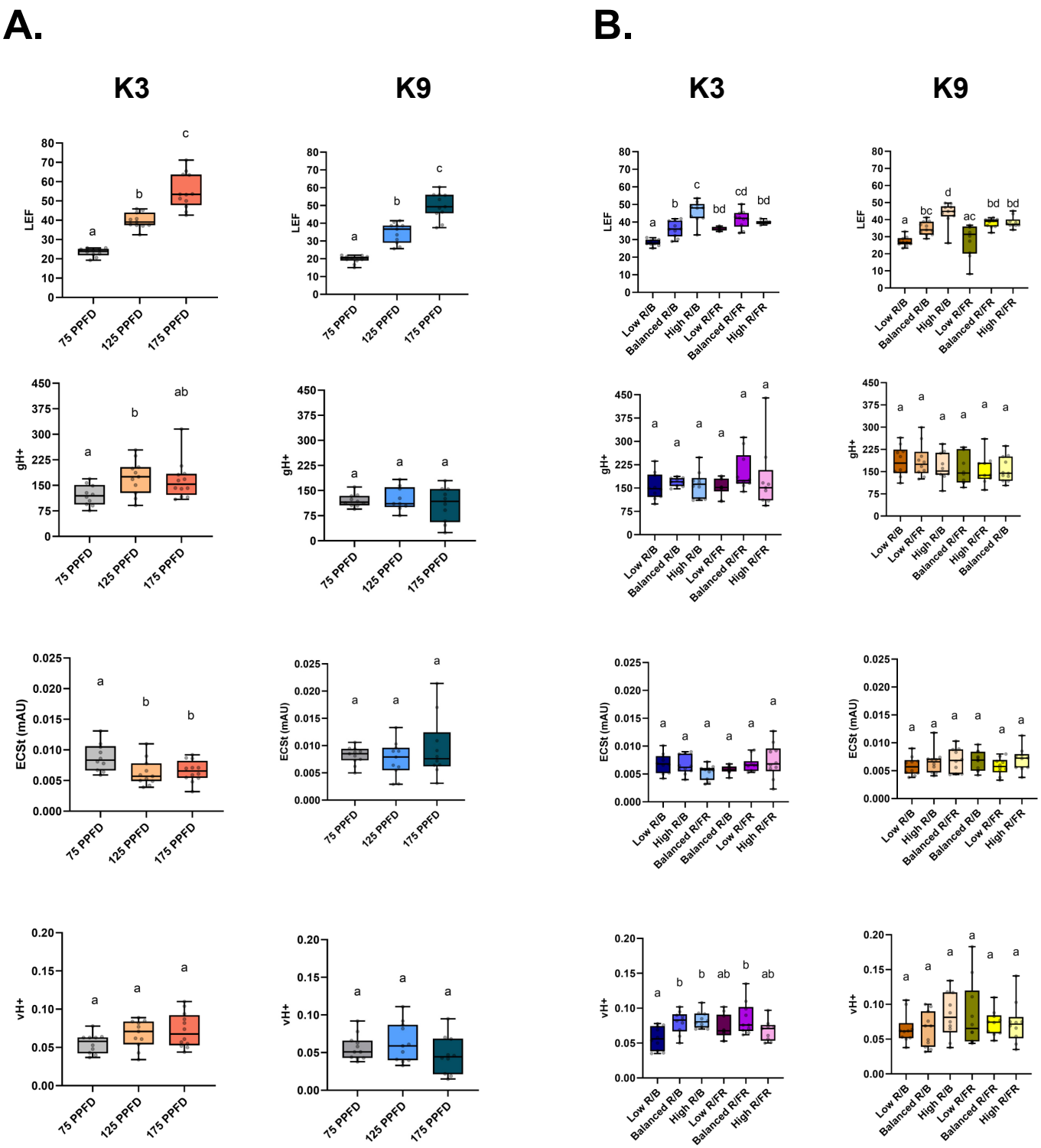

Supplemental Figure 2: Effect of Light Intensity and spectra on Photosynthetic Parameters Measured with MultispeQ.

A. Light intensity effect on photosynthetic parameters (LEF, gH+, ECSt, vH+) were measured with MultispeQ at 35 dpi (n=10).
B. Light spectra effect on photosynthetic parameters (LEF, gH+, ECSt, vH+) were measured with MultispeQ at 35 dpi (n=10).
Letters show significant differences using a one-way ANOVA and Tukey's post-hoc test (adjusted p-value < 0.05).

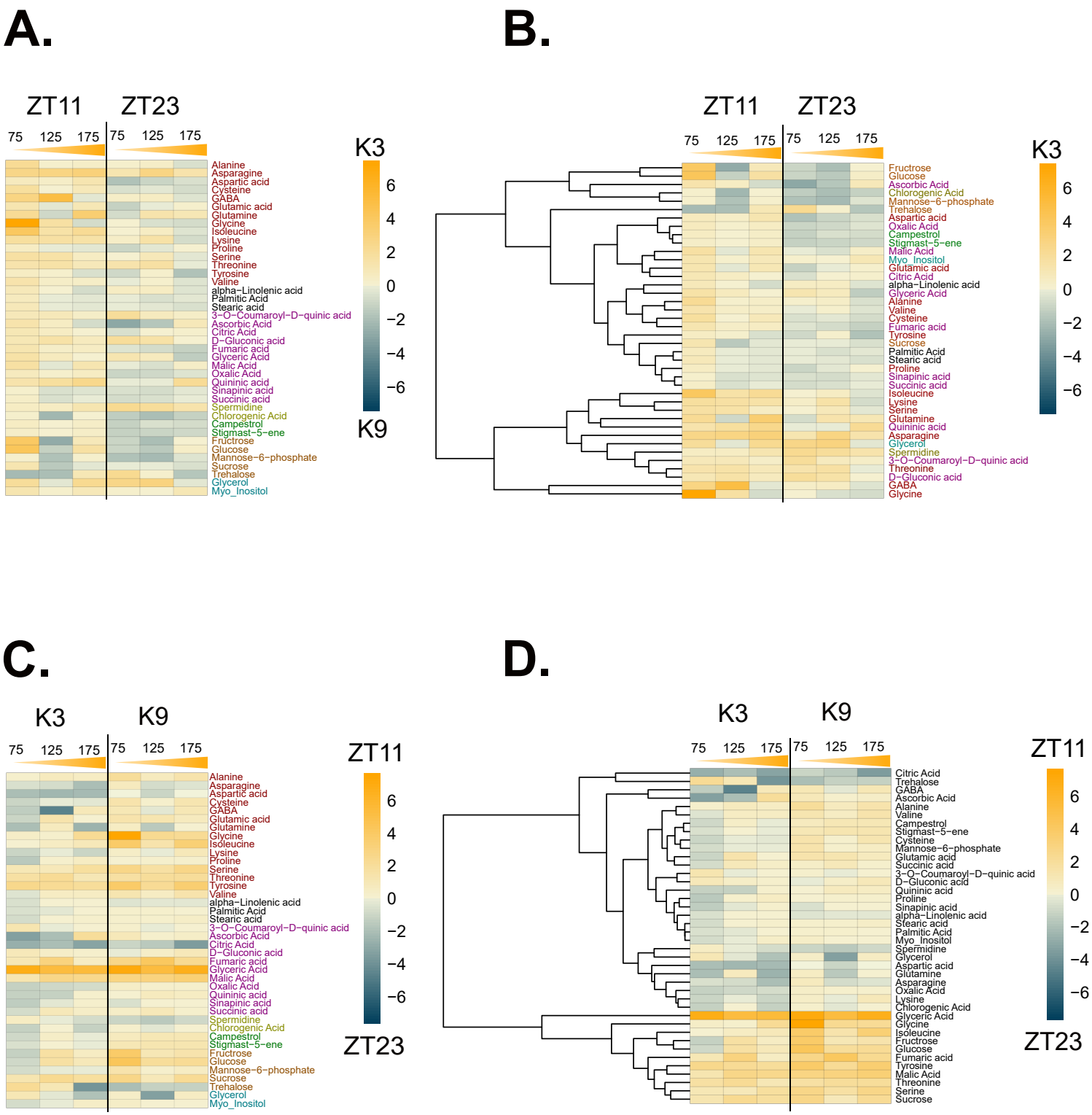

Supplemental Figure 3: GC-MS analysis of kale cultivars K3 and K9 under different light intensities (75 PPFD, 125 PPFD and 175 PPFD) and at different time of the day (ZT11 and ZT23).

A. Heatmap of relative cultivars metabolite changes at ZT11 and ZT23.
B. Eucledian distance clustered heatmap of relative cultivars metabolite changes.
C. Heatmap of relative diel metabolite changes in K3 and K9.
D.Eucledian distance clustered heatmap of relative diel metabolite changes in K3 and K9. Heatmaps were generated using the R package *Pheatmaps*. Scale represents Log2 fold-change (FC); n=4.

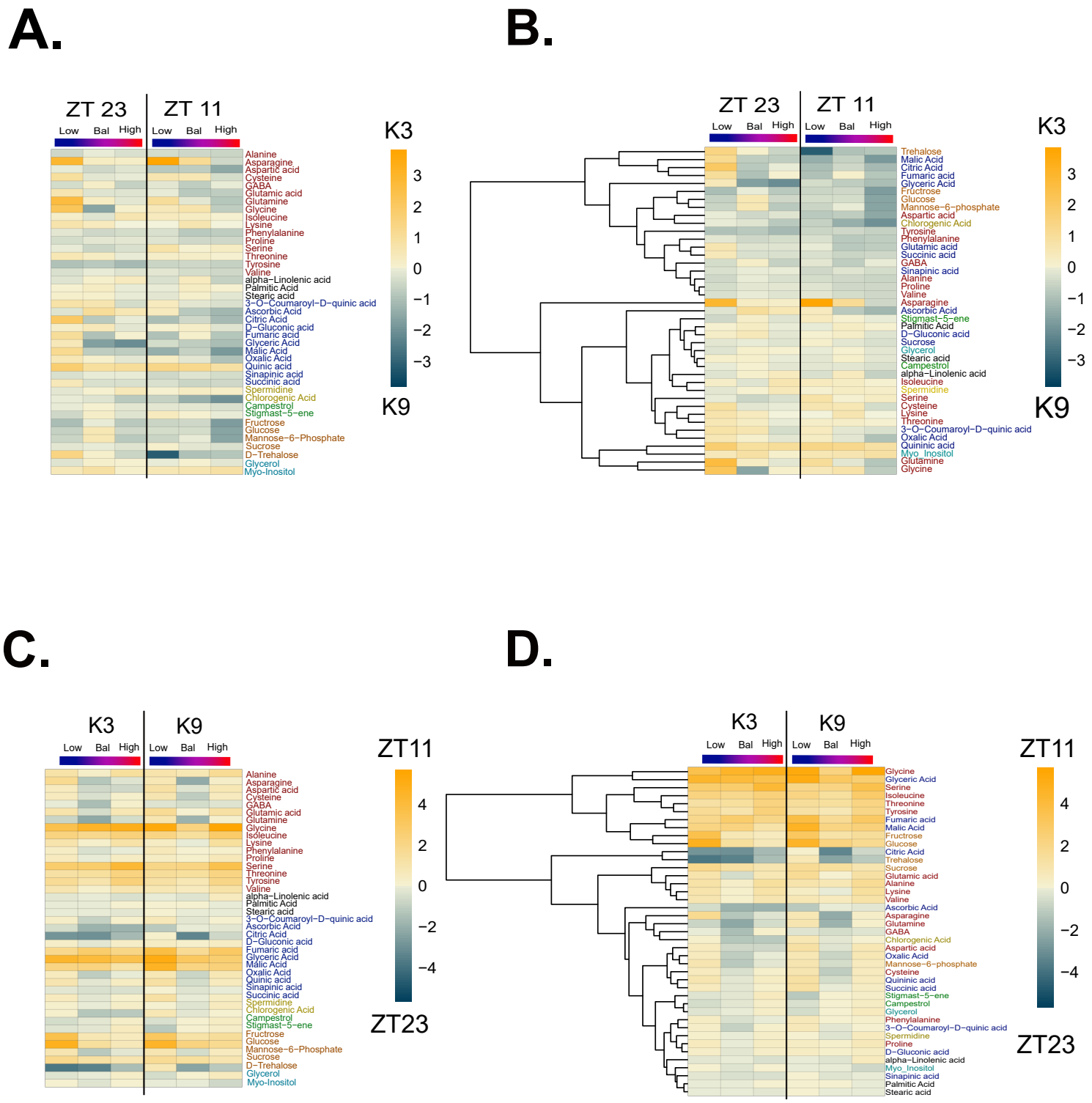

Supplemental Figure 4: GC-MS analysis of kale cultivars K3 and K9 under different light spectra (low, balanced, and high R/B ratios) and at different time of the day (ZT11 and ZT23).

A. Heatmap of relative cultivars metabolite changes at ZT11 and ZT23.
B. Eucledian distance clustered heatmap of relative cultivars metabolite changes.
C. Heatmap of relative diel metabolite changes in K3 and K9.
D. Eucledian distance clustered heatmap of relative diel metabolite changes in K3 and K9. Heatmaps were generated using the R package *Pheatmaps*. Scale represents Log2 fold-change (FC); n=4.

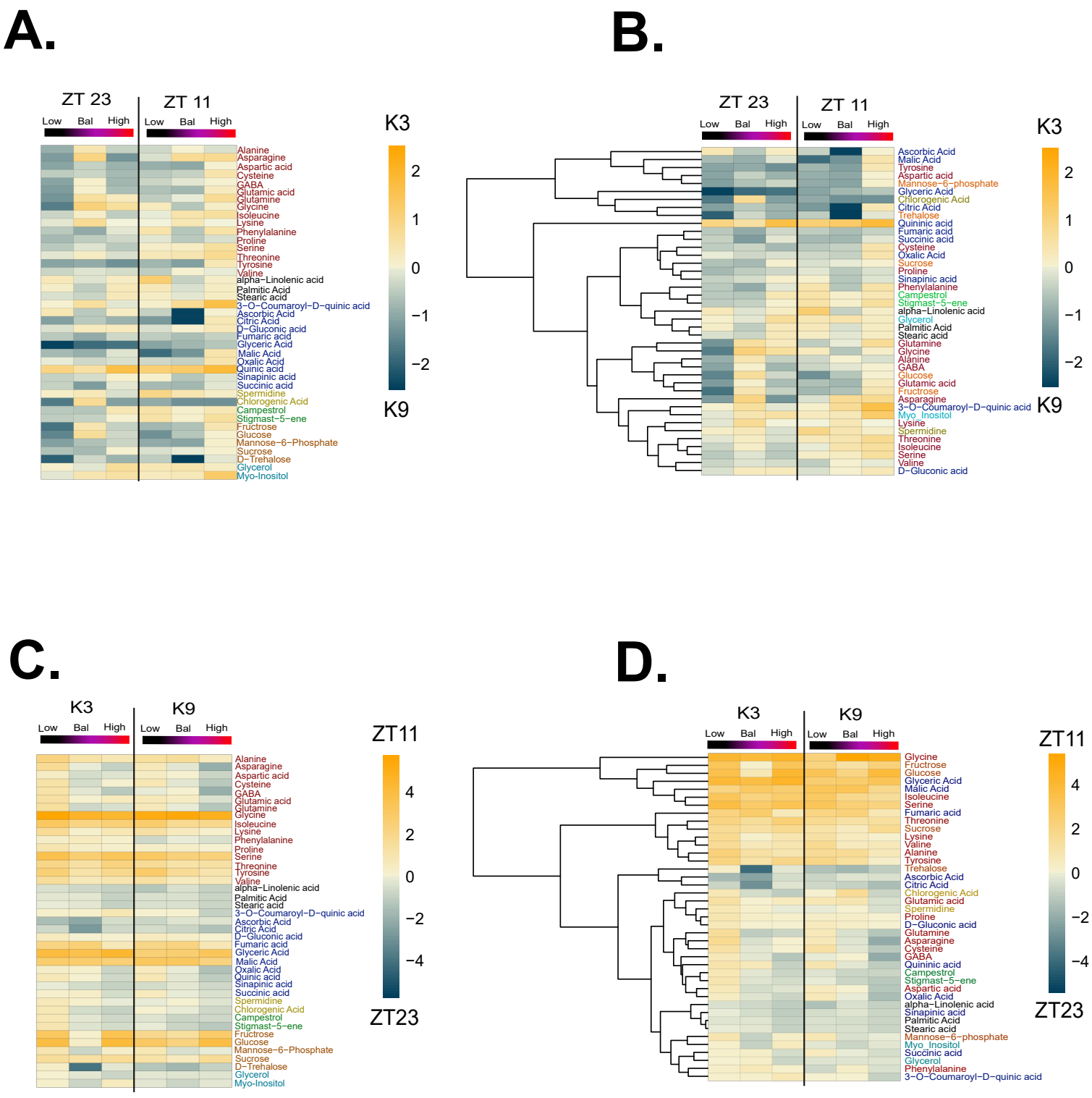

Supplemental Figure 5: GC-MS analysis of kale cultivars K3 and K9 under different light spectra (low, balanced, and high R/FR ratios) and at different time of the day (ZT11 and ZT23).

A. Heatmap of relative cultivars metabolite changes at ZT11 and ZT23.
B. Eucledian distance clustered heatmap of relative cultivars metabolite changes.
C. Heatmap of relative diel metabolite changes in K3 and K9.
D. Eucledian distance clustered heatmap of relative diel metabolite changes in K3 and K9. Heatmaps were generated using the R package *Pheatmaps*. Scale represents Log2 fold-change (FC); n=4.